Visual pathways in the brain of the jumping spider *Marpissa muscosa*

Running title: **Jumping spider visual pathways**

Philip O.M. Steinhoff[1*], Gabriele Uhl[1], Steffen Harzsch[2] & Andy Sombke[3]

[1] Zoological Institute and Museum, General and Systematic Zoology, University of Greifswald, Loitzer Straße 26, 17489 Greifswald, Germany

[2] Zoological Institute and Museum, Cytology and Evolutionary Biology, University of Greifswald, Soldmannstraße 23, 17489 Greifswald, Germany

[3] Department of Integrative Zoology, University of Vienna, Althanstraße 14, 1090 Vienna, Austria

[*]*Corresponding Author. E-Mail: philipsteinhoff@gmail.com*

ACKNOWLEDGEMENTS

The authors wish to thank Georg Brenneis and Matthes Kenning (University of Greifswald) as well as Nicholas J. Strausfeld (University of Arizona, Tucson) and Friedrich G. Barth (University of Vienna) for helpful discussions. We are grateful to Kerstin Stejskal and Thomas Hummel (Department of Neurobiology, University of Vienna) for providing *Cupiennius salei* and Elvira Lutjanov, Christian Müller, Sabine Ziesemer and Jan-Peter Hildebrandt (all University of Greifswald) for help with western blot analysis. Tim M. Dederichs and Peter Michalik (both University of Greifswald) helped to obtain pictures with the Visionary Digital camera system. Monica M. Sheffer provided helpful linguistic comments that improved the manuscript. This study was financially supported by the German Research Foundation DFG UH 87/11-1 and DFG INST 292/119-1 FUGG, DFG INST 292/120-1 FUGG. POMS was additionally supported by a Bogislaw scholarship from the University of Greifswald and a Laudier Histology cooperation & travel grant.

DATA AVAILABILITY STATEMENT

The data that support the findings of this study are available from the corresponding author upon reasonable request.

Abstract

Some animals have evolved task differentiation among their eyes. A particular example is spiders, where most species have eight eyes, of which two (the principal eyes) are used for object discrimination, whereas the other three pairs (secondary eyes) detect movement. In the spider species *Cupiennius salei* these two eye types correspond to two visual pathways in the brain. Each eye is associated with its own first and second order visual neuropil. The

second order neuropils of the principal eyes are connected to the arcuate body, whereas the second order neuropils of the secondary eyes are linked to the mushroom body. However, eye size and visual fields are considerably different in jumping spiders. We explored the principal- and secondary eye visual pathways of the jumping spider *Marpissa muscosa*. We found that the connectivity of the principal eye pathway is the same as in *C. salei*, while there are differences in the secondary eye pathways. In *M. muscosa,* all secondary eyes are connected to their own first order visual neuropils. The first order visual neuropils of the anterior lateral and posterior lateral eyes are further connected with two second order visual neuropils, whereas the posterior median eyes lack second order visual neuropils and their axons project only to the arcuate body. This suggests that the posterior median eyes probably do not serve movement detection in *M. muscosa.* Furthermore, the second order visual neuropil (L2) in *Marpissa muscosa* potentially integrates information from the secondary eyes and might thus enable faster movement decisions.

Keywords

Secondary eyes, principal eyes, visual pathway, jumping spider, visual neuropils, brain, *Marpissa muscosa*, RRID AB_528479, RRID AB_2637882, RRID AB_477585, RRID AB_1541510, RRID AB_2338680, RRID AB_2534074, RRID AB_2315147

1 Introduction

In some animal species with multiple eyes, different eyes serve different specific tasks, such as compound eyes and ocelli in insects or the rhopalia in box jellyfishes (Garm et al., 2007; O'Connor et al., 2009; Paulus, 1979). Spiders vary strongly in their visual abilities, as well as in number, arrangement and size of their eyes (reviewed in Morehouse et al. 2017). Most species possess four pairs of eyes, of which one pair differs from the three other pairs in its anatomy and developmental origin (Land, 1985a; Morehouse et al., 2017). The principal eyes (or anterior median eyes) possess a movable retina and their spectral sensitivities allow for color vision (Barth et al. 1993; Land, 1985b; Schmid, 1998; Yamashita & Tateda, 1976, 1978). The other three pairs of eyes are the so-called secondary eyes (posterior median, anterior lateral and posterior lateral eyes). Their morphology and anatomy differs considerably among spider families (Homann, 1952, 1950), but they generally do not have a movable retina. In several groups of cursorial hunting spiders, the secondary eyes are used for movement detection (Land, 1985a; Morehouse et al., 2017; Schmid, 1998). Most secondary eyes possess

a light-reflecting tapetum (but absent in e.g. jumping spiders), which led to the assumption that they play a major role for night or dim light vision (Foelix, 1996).

Jumping spiders (Salticidae) are cursorial hunters with excellent vision. Their eyes have been studied in much greater detail compared to any other spider group (e.g. Harland et al., 2012; Land, 1985a; Morehouse et al., 2017). The principal eyes of jumping spiders are large and face forward; their field of view is small, but their spatial acuity is one of the highest among invertebrate eyes (Harland et al., 2012; Land, 1985b, 1985a). The secondary eyes of salticids possess only one photoreceptor type and thus cannot discriminate colors (Yamashita and Tateda, 1976). Among the secondary eyes, the anterior lateral eyes (ALE) and posterior lateral eyes (PLE) are large, able to detect motion, and elicit an orienting response of the principal eyes towards the moving object (Duelli, 1978; Jakob et al., 2018; Spano et al., 2012; Zurek et al., 2010; Zurek and Nelson, 2012a, 2012b). The posterior median eyes (PME) of most salticids (except for the non-salticoids) are very small and positioned between ALE and PLE (Land, 1985b; Maddison and Hedin, 2003). Since the fields of view of ALE and PLE overlap, the PME do not have an exclusive field of view (Land, 1985b).

While the eyes of jumping spiders have been studied in detail, less is known about the brain structures that process visual information (Duelli, 1980; but see Hanström, 1921; Hill, 1975; Nagata et al., 2019; Steinhoff et al., 2017; Strausfeld, 2012). Our knowledge on the visual processing pathways in the brain of spiders is mostly based on investigations of the spider model species *Cupiennius salei* (Keyserling, 1877) (Babu and Barth, 1984; Becherer and Schmid, 1999; Schmid and Duncker, 1993; Strausfeld et al., 1993; Strausfeld and Barth, 1993). *C. salei* possesses two separate visual pathways, one for the principal eyes and one for all secondary eyes (Strausfeld et al., 1993; Strausfeld and Barth, 1993). In *C. salei*, every eye is connected to its own first and second order visual neuropil (Barth, 2002). While the second order visual neuropils of the principal eyes are connected to the arcuate body (Strausfeld et al., 1993), the second order visual neuropils of the secondary eyes are associated with the mushroom bodies (Strausfeld and Barth, 1993). Additionally, the first order visual neuropils of the secondary eyes are directly connected to the arcuate body (Babu and Barth, 1984).

In *C. salei,* similar to salticids, the principal eyes are used for object recognition, while the secondary eyes serve the purpose of movement detection (Fenk, Hoinkes, & Schmid, 2010; Schmid, 1998). The secondary eyes of *C. salei* have a high spectral sensitivity, similar to their principal eyes (Barth et al., 1993) and similar to jumping spiders are capable of acute motion detection (Fenk & Schmid, 2010; Zurek & Nelson, 2012b). However, they are unable to detect

color in moving objects (Orlando and Schmid, 2011) and the relative size of different eyes and thus fields of view in *C. salei* differ considerably from jumping spiders (Land, 1985b; Land and Barth, 1992). Furthermore, Steinhoff et al. (2017) showed that the structure and arrangement of the secondary eye visual neuropils in the jumping spider *Marpissa muscosa* (Clerck, 1757) differ from those in *C. salei.* We thus hypothesize, that the secondary eye visual pathways of jumping spiders also differ from that in the model species *C. salei.* Here, we describe the principal and secondary eye visual pathways in the brain of the jumping spider *M. muscosa*. We use paraffin histology, immunohistochemistry, and microCT analysis to visualize tracts in the visual system. We compare our findings in *M. muscosa* with results of earlier studies and new immunohistochemical data on the principal and secondary eye pathways in the brain of *C. salei*. We discuss the similarities and differences in the principal and secondary eye pathways of these two spider species in the light of different functional roles of their eyes.

2 Material and Methods

2.1 Animals

Adult female *Marpissa muscosa* were collected in and near Greifswald (Germany). Spiders were fed on *Drosophila* sp. weekly and kept individually in plastic boxes of 145 x 110 x 68 mm size that were enriched with paper tissue.

2.2 Paraffin-histology

The prosomata of two females of *M. muscosa* were fixed in Gregory's artificially aged Bouin solution (Gregory, 1980). After four days in fixative, the prosomata were dehydrated through a graded ethanol series (80%, 90%, and 3x 96% ethanol for 20 minutes each) and were then transferred for two hours into a 1:1 solution of 96% ethanol:tetrahydrofuran (Carl Roth, CP82.1) at room temperature. Samples were kept for 24 hours in pure tetrahydrofuran followed by 24 hours in a solution of 1:1 tetrahydrofuran and paraffin (Carl Roth, 6643.1) at 60°C. Afterwards, samples were transferred to 100% paraffin at 60°C for 48 hours and then embedded in fresh paraffin. Sagittal and transversal sections (5 µm) were cut with a motorized rotary microtome (Microm HM 360). Sections were stained with Azan according to Geidies (Schulze and Graupner, 1960), and mounted in Roti-Histokitt II (Carl Roth, T160.1).

2.3 MicroCT analysis

140 Prosomata of two individuals of *M. muscosa* and one individual of *C. salei* were fixed in
141 Dubosq–Brazil solution (1 g saturated alcoholic picric acid, 150 ml 80% ethanol, 15 ml pure
142 acetic acid, and 60 ml 37% formaldehyde). Prior to fixation, legs and opisthosomata were cut
143 off and cuticle and musculature were removed from the dorsocaudal part of the prosomata
144 to allow faster penetration of the fixative. After four days in fixative, samples were washed
145 six times for 20 minutes in 0.1 M phosphate buffered saline (PBS, pH 7.4) followed by
146 dehydration in a graded ethanol series (80%, 90%, 96% and 3x 99,8% ethanol for 20 minutes
147 each). Samples were then transferred to an 1% iodine solution (iodine, resublimated [Carl
148 Roth, X864.1] in 99.8% ethanol) over 48 h to enhance tissue contrast (Sombke et al., 2015)
149 and subsequently critical point dried with an automated dryer (Leica EM CPD300). The
150 protocol applied was: slow CO_2 admittance with a delay of 120 seconds, 30 exchange cycles,
151 followed by a slow heating process and slow gas discharge. Dried prosomata were mounted
152 using a conventional glue gun onto aluminum rods, so that the anterior median eyes were
153 oriented upwards.
154 MicroCT scans were performed using a Zeiss XradiaXCT-200 (Sombke et al., 2015). Scans were
155 performed with a macro-, a 4x- and a 20x objective lens unit and the following settings: 40 kV
156 and 8 W or 30 kV and 6 W, 200 µA, exposure times between 2 and 4 s. Tomographic
157 projections were reconstructed with the XMReconstructor software (Zeiss), resulting in image
158 stacks (TIFF format). Scans were performed using Binning 2 for noise reduction and were
159 reconstructed with full resolution (using Binning 1).
160
161 **2.4 Immunohistochemistry**
162 Four different combinations of markers were used to visualize neuropils and connecting
163 neurites in the visual system (see Table 1 for a list of marker combinations used, and Table 2
164 for specifications of labeling reagents).
165 After anaesthetization with CO_2, brains of 31 females of *M. muscosa* (details Tab. 2) and four
166 females of *C. salei* were dissected in PBS and fixed in 4% paraformaldehyde over night at room
167 temperature. Specimens for histamine immunohistochemistry were prefixed overnight at 4°C
168 in 4% N-(3-Dimethylaminopropyl)-N'-ethylcarbodiimide hydrochloride (EDAC, Sigma–Aldrich
169 E6383). Brains were washed six times for 15 minutes each in PBS and subsequently immersed
170 in Poly-L-Lysin (Sigma-Aldrich, P4707) for one minute. Samples were then embedded in 4%
171 agarose (Sigma-Aldrich, A9414) and sectioned (50 or 80 µm) with a Microm HM 650 V
172 vibratome. After permeabilization in PBS-TX (PBS, 0.3% Triton X-100 [Sigma-Aldrich, X100], 1

173 % bovine serum albumin [Sigma-Aldrich, A2153], 0.05% Na-acide; or alternatively PBS, 0.5%
174 Triton, 1.5% DMSO) for 1 h at room temperature, incubation in primary antibodies took place
175 over night at 4°C or room temperature. Sections were washed in several changes of PBS-TX
176 after the incubation. Incubation in secondary antibodies or counterstains took place
177 overnight at 4°C or room temperature. After washing in several changes of PBS, sections were
178 mounted in Mowiol (Merck 475904).
179
180 The brains of five additional females of *M. muscosa* were processed as whole-mounts, using
181 an adjusted protocol after Ott (2008) (see also Steinhoff et al., 2017). Brains were dissected
182 in TRIS buffer (0.1 M, pH 7.4 [Carl Roth, 4855]), and fixed in zinc-formaldehyde at room
183 temperature under soft agitation for several days. Afterwards, brains were washed in TRIS
184 buffer three times for 15 minutes each and incubated in a 4:1 mixture of methanol and DMSO
185 (Dimethylsulfoxide [Carl Roth, 4720]) for 2 h. After incubation in 100% methanol for 1 h,
186 brains were rehydrated in a graded series of methanol (90%, 70%, 50%, 30%) for 10 minutes
187 each and washed in TRIS buffer. This was followed by permeabilization in PBS-DMSO (PBS, 5%
188 bovine serum albumin, 1% DMSO, 0.05% Na-acide) for 2 h at room temperature and
189 incubation in primary antibody for 4 days at 4°C. Brains were then washed several times for
190 2 h in PBS-DMSO and incubated in secondary antibody for 4 days at 4°C, and transferred to a
191 graded series of glycerol, with 1%, 2%, 4% (for two hours each) and 8%, 15%, 30%, 50%, 60%,
192 70%, 80% (for one hour each) glycerol in TRIS buffer and 1% DMSO. After five changes in pure
193 ethanol for 30 minutes each, brains were mounted in fresh methyl salicylate (Sigma, 76631).
194 In control experiments, in which we replaced the primary antibodies with PBS-TX, no neuronal
195 labeling was detected.
196
197 **2.5 Western Blot**
198 In western blots of *Drosophila melanogaster* Meigen, 1830 head homogenates (Klagges et al.,
199 1996), the monoclonal antibody mouse anti-*Drosophila* synapsin ‘‘Synorf 1‘‘ (provided by E.
200 Buchner, Universität Würzburg, Germany; raised against a *Drosophila* Glutathione S-
201 Transferase(GST)-synapsin fusion protein) recognizes at least 4 synapsin isoforms (ca. 70, 74,
202 80, and 143 kDa). In western blot analyses in Crustacea (Harzsch and Hansson, 2008; Sullivan
203 et al., 2007) and Chilopoda (Sombke et al., 2011), isoforms in the same range (75-90 kDA)
204 were recognized. Furthermore, the Synorf 1 antibody labels synaptic neuropil in taxa as
205 diverse as Araneae (Fabian-Fine et al., 1999; Nagata et al., 2019; Steinhoff et al., 2017;

206 Widmer et al., 2005), Chaetognatha (Harzsch and Müller, 2007) and Plathelminthes (Cebrià,
207 2008), suggesting that the epitope that this antiserum recognizes is highly conserved. To test
208 this, we conducted a western blot analysis as well, in which we compared brain tissue of *D.*
209 *melanogaster* and *M. muscosa*. The antibody provided similar results for both species,
210 staining one strong band around 70 kDa, and in *M. muscosa* another weak band around 60
211 kDa. This result suggests that the epitope that Synorf 1 recognizes is conserved between *D.*
212 *melanogaster* and *M. muscosa*.
213
214 **2.6 Microscopy, image processing and nomenclature**
215 Immunohistochemically labelled sections and whole-mounts were examined and
216 photographed with a Leica SP5 II confocal microscope (cLSM). Paraffin sections were
217 examined and photographed with a customized Visionary Digital BK Plus Lab System
218 (duninc.com/bk-plus-lab-system.html). 3D-visualization of microCT image stacks was
219 prepared in AMIRA 6.0.0 (ThermoFisher). An interactive 3D-visualization of the microCT
220 reconstructions was created using ImageJ 1.51n and Adobe Acrobat Pro 9.0 (see supporting
221 information; Figure S1). Images were processed in Corel PaintShop Pro using global contrast
222 and brightness adjustment features as well as black and white inversion. Schematic drawings
223 were generated using Corel Draw 20.1 and figure plates were assembled in Corel PaintShop
224 Pro 21.0. A color code for all depicted structures, as used in Loesel et al. (2013) and Steinhoff
225 et al. (2017), was used for 3D visualizations and the schematic drawings. The terminology
226 used for brain structures follows Richter et al. (2010). For structures specific to spiders, we
227 use terms according to Lehmann et al. (2016), Strausfeld et al. (1993) and Strausfeld and Barth
228 (1993). Positional information is given with respect to the body axis. We are referring to
229 results from immunohistochemical experiments as immunoreactivity, e.g. synapsin-
230 immunoreactivity.
231
232 **Abbreviations**
233
234 **AB** Arcuate body
235 **ALE** Anterior lateral eyes
236 **AL1** First order visual neuropils of ALE
237 **AL2/PL2** Second order visual neuropils of ALE and PLE
238 **AL1x** Neuropilar subunit of the AL1
239 **AME** Anterior median eyes
240 **AM1** First order visual neuropils of AME
241 **AM2** Second order visual neuropils of AME
242 **L2** Second order visual neuropils of anterior and posterior lateral eyes
243 **MB** Mushroom bodies (neuropil with attributes of a mushroom body-like organization)
244 **MBbr** Mushroom body bridge

MBn	Neurites between pedunculus and AL2/PL2
MBh	Mushroom body haft
MBp	Pedunculus of the mushroom body
MBs	Mushroom body shaft
PLE	Posterior lateral eyes
PL1	First order visual neuropils of the PLE
PL1x	Neuropilar subunit of the PL1
PME	Posterior median eyes
PM1	First order visual neuropils of the PME
PM2	Second order visual neuropils of the PME
SC1-3	Protocerebral soma cluster 1-3

3 Results

3.1 General organization of the protocerebrum

In *Marpissa muscosa,* the protocerebrum comprises bilaterally paired neuropils of the visual system and the mushroom body as well as the unpaired arcuate body and the protocerebral neuropil (Figs. 1, 2; for details see Steinhoff et al., 2017). All neuropils of the visual system are recognizable in paraffin sections (Fig. 3) and microCT analysis (Fig. 4; supporting information, Fig. S1), and are also characterized by a strong synapsin-immunoreactivity (Figs. 1; 5; 6; 7a, b). Tracts and individual neurites exhibit prominent tubulin-immunoreactivity (Figs. 1; 2; 5; 6; 7). Furthermore, the optic nerves (between retinae and first order visual neuropils) and the corresponding first order visual neuropils display histamine- immunoreactivity (Fig. 8), which is known to consistently label retinula cell axons and their terminals in the visual systems of arthropods (Battelle et al., 1991; Harzsch et al., 2006; Harzsch, Wildt, Battelle, & Waloszek, 2005; Nässel, 1999; Schmid & Duncker, 1993; Sombke & Harzsch, 2015). A soma cortex including three discernable protocerebral clusters surrounds most of the central nervous system (CNS) (Figs. 2; 5a; 6a-b, d; 7a–d). Soma cluster 1 (SC1) is located between the first order visual neuropils of the lateral eyes and the second order visual neuropil of anterior lateral and posterior lateral eyes (AL2/PL2), cluster 2 (SC2) medially to the AL2/PL2, and cluster 3 (SC3) anteromedially to the mushroom body bridge (MBbr) (Fig. 2).

3.2 The principal eye pathway

The retina of the anterior median eyes (AME) is connected to its first order visual neuropil (AM1), which consists of at least two, but most likely four tightly adjoining subunits (Fig. 1a,e,f). The AM1 is situated close to the second order visual neuropil of the AME (AM2) and connected to it *via* parallel neurites (Fig. 1e,f). The AM2 is large, oval shaped and its posterior margin within the protocerebral neuropil is not clearly recognizable in anti-synapsin labeling (Fig. 1). Anti-tubulin labeling reveals a tract of neurites that connects the AM2 with the lateral

283 flanges of the AB, as well as some neurites with unclear termination that penetrate the
284 protocerebral neuropil (Fig. 1c-e).
285
286 **3.3 Connectivity of the first order visual neuropils of the anterior and posterior lateral eyes**
287 The retinae of the anterior lateral eyes (ALE) and posterior lateral eyes (PLE) are connected
288 with their respective first order visual neuropils (AL1 and PL1) *via* short, thick optic nerves
289 (Figs. 3b, c; 4a-b; 5c). A subpopulation of histaminergic neurites, which are interpreted here
290 as retinula cell axons, terminates in distinct distal layers of these neuropils (AL1x and PL1x;
291 Fig. 8a–c). Both the AL1 and PL1 are connected to the second order visual neuropil of the
292 lateral eyes (L2) and the AL2/PL2 *via* prominent tracts of parallel ordered neurites that exhibit
293 strong tubulin-immunoreactivity (Figs. 2; 5c; 6a-b, d; 7a-b). This connectivity is also evident in
294 both, histological sections (Fig. 3) and microCT analysis (Fig. 4). The tracts are predominantly
295 formed by neurites that originate in SC1, which surrounds this region of the anterior
296 protocerebrum laterally, dorsally and medially (Figs. 2; 6a-b; 7b, d). The L2 and the AL2/PL2
297 are bi-lobed, which corresponds to the separate inputs from AL1 and PL1 (Figs. 3a; 3b, d; 5a;
298 6a, C; 8a, b). In histological sections, a thin but conspicuous tract is detectable that passes
299 between L2 and AL2/PL2 and likely terminates in the arcuate body (AB) (Figs. 3b, c; 5a, b; 6d;
300 7b). The neurites forming this tract might originate in SC1 and further innervate the AL1x and
301 PL1x, as well as the PM1 (see below; Figs. 3; 5a, b; 6d).
302
303 **3.4 Connectivity of the first order visual neuropils of the posterior median eyes**
304 The posterior median eyes (PME) are much smaller than all three other pairs of secondary
305 eyes, and so is their retina (Fig. 4c, e). Because of the small retina, only a thin but long nerve,
306 which enters the protocerebrum between the AL1 and PL1, connects the PME to its first order
307 visual neuropil (PM1) (Figs. 4e; 6c, c'). The PM1 is situated between AL1 and PL1 (Figs. 3a-b;
308 4e, 5b; 6c-d; 7b; 8a). A prominent tract projects from the PM1 to the dorsoventral part of the
309 protocerebrum and seems to terminate in the anterolateral apices of the AB (Fig. 3b; 5b; 6d).
310
311 **3.5 The second order visual neuropil of ALE and PLE and the mushroom body**
312 The second order visual neuropil of ALE and PLE (AL2/PL2) is of glomerular organization and
313 composed of two lobes that tightly adjoin dorsally and are fused in their ventral part (Figs. 7a,
314 c, d; 9a-b). Thus, only a uniform array of glomeruli is visible in most sections (Figs. 3b; 4a, c,
315 e; 5; 6). Each glomerulus is composed of a high number of synaptic complexes (Fig. 9c–e).

316 These synaptic complexes can be visualized by anti-synapsin labeling and phalloidin-labeling
317 (Fig. 9d, e). Co-localization of synapsin and phalloidin is almost absent (Fig. 9). Individual
318 glomeruli are innervated by neurites originating in the AL1 and PL1 (Figs. 5c; 6a, b, d; 7d).
319 Anti-tubulin labeling reveals that neurites interweave the array of glomeruli mostly in parallel
320 from proximal to distal (Fig. 5c; 6a). Within the core-region of the AL2/PL2, tubulin-
321 immunoreactive neurites are more abundant (Fig. 6a,c. Two neurite bundles (MBn) connect
322 the AL2/PL2 and the mushroom body pedunculus (MBp) and form a distinct chiasm close to
323 the AL2/PL2 (Figs. 7a, c, d; 9a). Neurites from the medial SC2 contribute to these bundles by
324 projecting into the AL2/PL2 and into the MBp (Figs. 2; 6a-c; 7a, d). Other neurites from SC2
325 pass between AL2/PL2 and MBp towards the L2 (Fig. 6b, d). Thus, a large number of
326 interweaving neurites characterizes the region of the MBn, which makes tracing of individual
327 trajectories difficult (Fig. 7a, d).
328 Some long neurites that appear to originate in SC2 project along the periphery of the MBp
329 and join with neurites arising from the mushroom body haft (MBh). Together they form the
330 mushroom body bridge (MBbr) (Figs. 2; 6c; 7a, c, d). Other peripheral neurites from SC2 enter
331 the MBh, where they seem to terminate (Figs. 2; 4b, d, f; 7d)
332
333 **3.6 Visual neuropils and the mushroom body in *Cupiennius salei***
334 The dorsalmost neuropils in the protocerebrum of *C. salei* are the AM1 and AM2, which are
335 connected by numerous intertwining neurites (Fig. 10a). The AM2 is connected to the AB *via*
336 a thin tract (Fig. 10a). Located ventrally and somewhat anterior to the AM1 is the PM1, which
337 is large and spans over one hemisphere of the protocerebrum at its broadest part (Fig.
338 10a,b,e). Its shape is cup-like, but somewhat irregular (Fig. 10e). The PL1 is situated
339 anterioventral of the PM1, is similar in size, but horseshoe shaped (Fig. 10b). Both the PM1
340 and the PL1 are subdivided into an upper, strongly synapsin-immunoreactive part where the
341 retinula cell axons terminate and a lower part where the synapsin-immunoreactivity is more
342 patchily distributed (PM1x and PL1x; Fig. 10b,e). Tubulin-immunoreactivity is strongest in the
343 lower part, where the neurites that connect the PM1 and PM2 with their respective second
344 order neuropils bundle together. The AL1 is the smallest first-order neuropil and located close
345 to the midline, between PM1 and PL1 (Fig. 10b). Each first order visual neuropil is connected
346 to its second order visual neuropil. These are of glomerular organization and situated close to
347 each other (Fig. 10b,c). While the AL2 is horseshoe shaped, the PL2 and PM2 are more
348 elongate in shape and also larger (Fig. 10b,c).

349 The mushroom body is characterized by strong synapsin-immunoreactivity and consists of a
350 pedunculus (MBp), a shaft (MBs) and a haft (MBh) (Fig. 10b). The MBs and the MBh are fused
351 with the MBp, and together form one continuous synapsin-immunoreactive domain (Fig.
352 10b).
353

354 # 4 Discussion

355 Comparative neuroanatomical studies on different spider species show that while general
356 brain anatomy is similar, the structure of different neuropils especially within the
357 protocerebrum varies (Hanström, 1921; Long, 2016; Steinhoff et al., 2017; Weltzien and
358 Barth, 1991). The previous investigation by Steinhoff et al. (2017) on the general brain
359 anatomy of *Marpissa muscosa* suggested that the brains of jumping spiders and the spider
360 species *Cupiennius salei* differ in structure and arrangement of neuropils. Although the
361 general architecture is similar, we have shown here that the connectivity of neuropils in the
362 secondary eye pathways differ between these two species, which suggests differences in
363 information processing and function of secondary eye visual neuropils.
364 The relative size and position of the secondary eyes differs between *M. muscosa* and *C. salei.*
365 While in *M. muscosa* the PME is very small and oriented sideways, it is the largest eye in *C.*
366 *salei* and oriented forward (Morehouse et al., 2017; Fig. 11). The PLE are similar in relative
367 size and position, but the ALE are considerably smaller in *C. salei,* albeit also oriented forward
368 (Fig. 11). The relative size of the retinae as well as the brain is smaller in *C. salei*, which is why
369 the optic nerves associated with the eyes are much longer in *C. salei* (Fig. 11).
370

371 **4.1 Connectivity of neuropils in the principal eye pathway**

372 The connection of the AME retinula cell axons to the AM1 has recently been described in
373 detail by Nagata et al. (2019) for the jumping spider *Hasarius adansoni*. These authors
374 revealed that there are four photoreceptor layers in the retina, which each connect to one of
375 four subregions in the AM1 (Nagata et al., 2019). We show here, that *in M. muscosa* the AM1
376 is further connected to the AM2, which is the same as described for *C. salei* (Strausfeld et al.,
377 1993). In *C. salei*, two types of neurons have been identified whose axons connect the AM2
378 with the flanges and the inner part of the AB (Strausfeld et al., 1993). In *M. muscosa* this
379 pattern is likely the same, although we were only able to unambiguously detect neurites that
380 connect the AM2 with the flanges of the AB. There are, however, neurites that project from

381 the AM2 into the protocerebral neuropil and some of those may well proceed towards the
382 inner part of the AB.
383
384 **4.2 Connectivity of the first order visual neuropils of the anterior and posterior lateral eyes**
385 In *M. muscosa*, all retinula cell axons from ALE, PLE and PME seem to terminate in their
386 associated first order visual neuropils (Fig. 8). This is in accordance to what has been found in
387 other Araneae (Becherer and Schmid, 1999; Duelli, 1980; Schmid and Duncker, 1993;
388 Strausfeld et al., 1993; Strausfeld and Barth, 1993). Nevertheless, this pattern is different in
389 all other investigated taxa of Chelicerata (e.g. Scorpiones, Xiphosura, or Pycnogonida), where
390 a subset of retinula cell axons also projects into the second order visual neuropils (Battelle,
391 Sombke, & Harzsch, 2016; Lehmann & Melzer, 2013, 2018). It should be noted, however, that
392 this discrepancy between spiders and all other arachnids still needs to be scrutinized using
393 cobalt fills, which have not been employed in spiders yet (Lehmann and Melzer, 2018). In *C.*
394 *salei*, a few histaminergic neurites terminate in all second order visual neuropils, and have
395 been interpreted as interneurons (Schmid and Duncker, 1993). However, as long as no
396 neuronal tracings have been carried out, it cannot be ruled out that these neurites might
397 instead represent retinula cell axons. In *M. muscosa*, we did not detect any histaminergic
398 neurites that terminate in the second order visual neuropils. There are, however, numerous
399 histaminergic neurites that terminate in AL1x and PL1x and we interpret those as retinula cell
400 axons.
401 In our histological sections, it appears as if some neurites that contribute to the tract between
402 AL1, PL1 and the AB, arise in AL1x and PL1x respectively (Fig. 3b, c; 5a-b). Hill (1975) described
403 in *Phidippus sp.* that neurites from the AL1x domain contribute to a tract projecting towards
404 the posterior protocerebrum. However, Hill (1975) did not mention terminations of retinula
405 cell axons in the AL1x and PL1x, but detected neurites connecting the AL1 with the AL1x. Thus,
406 it is possible that Hill (1975) either misinterpreted retinula cell axons as interneurons, or that
407 we missed connecting neurites between AL1 and AL1x. In our immunohistological
408 investigations, we found that synapsin-immunoreactive substructures of first order visual
409 neuropils are also present in *C. salei*, the PM1x and the PL1x. In both, *M. muscosa* and *C. salei,*
410 this region is additionally characterized by strong tubulin-immunoreactivity. This can be
411 explained by the tight packing of neurites that converge at the level of the AL1x and PL1x in
412 *M. muscosa* and the PM1x and PL1x in *C. salei* to form the tracts to the respective second
413 order visual neuropils. A subdivision of PM1 and PL1 is also visible in histamine-

414 immunolabeled material from the study by Schmid & Duncker (1993; compare Figs. 2c,d and
415 3a,b), although not discussed by the authors. It remains open whether retinula cell axons or
416 interneurons terminate at the synapsin immunoreactive part of the PL1x and PM1x in *C. salei*
417 and the AL1x and PL1x in *M. muscosa*.
418 In *M. muscosa*, the convoluted first order visual neuropils of the ALE and the PLE are both
419 connected with the AL2/PL2 and the L2, as well as with the AB, which is only partially
420 consistent with Hill's (1975) study on the nervous system in *Phidippus* spp., where he found
421 that axons of the AL1, and not the PL1, join the tract that projects towards the AB. Duelli
422 (1980), did not detect connections between PL1 and L2 in the salticids *Evarcha arcuta* (Clerck,
423 1757) and *Pseudamycus validus* (Thorell, 1877). He described "large field horizontal neurons,"
424 closely bypassing the AL2/PL2 and L2 and connecting the PL1 with the posterior
425 protocerebrum (Duelli, 1980). Judging from their structure and position, these neurons might
426 be identical with the neurites described in our study which contribute to the tract that
427 connects the first order visual neuropils of the secondary eyes with the arcuate body. This
428 discrepancy might be due to incomplete staining in the earlier studies where reduced-silver
429 staining was employed. Our approach combines specific and broader markers with specific
430 staining techniques. It should also be noted that the studies on the secondary eye pathways
431 in jumping spiders were conducted on different species. However, it seems unlikely that the
432 secondary eye pathways differ considerably within salticoid jumping spiders (Maddison and
433 Hedin, 2003; Morehouse et al., 2017).
434 Based on our results, AL2/PL2 and L2 are shared second order visual neuropils of both AL1
435 and PL1 in *M. muscosa*. The situation in *C. salei* is, however, different. Here, the first order
436 visual neuropils of all three secondary eyes are connected to individual second order visual
437 neuropils (compare Fig. 11a and b) (Strausfeld and Barth, 1993). Each of these second order
438 visual neuropils (AL2, PL2, PM2) is composed of small neuropilar glomeruli (compare Fig. 11).
439 An unstructured second order visual neuropil (without glomeruli), such as the L2, is absent in
440 *C. salei* (Strausfeld and Barth, 1993). Similar to the "giant interneurons" described for jumping
441 spiders by Duelli (1980), Strausfeld & Barth (1993) detected "lamina wide-field neurons" that
442 connect all first order visual neuropils with a region close to the AB. It is very likely that these
443 neurons correspond to the axons forming the tract between first order visual neuropils and
444 the AB that we described in *M. muscosa*.
445
446 **4.3 First order visual neuropils of the posterior median eyes**

447 The PM1 is by far the smallest first order visual neuropil of all secondary eyes in *M. muscosa*.
448 This correlates with the much smaller overall size of the PME (compared to ALE and PLE). The
449 PME have previously been considered vestigial (Land, 1985a, 1972), but since there is an optic
450 nerve and a corresponding first order visual neuropil, we conclude that these eyes are
451 functional. Previously, Steinhoff et al. (2017) considered the PM1 to be a second order visual
452 neuropil ("PM2"), based on its close spatial relationship with the AL1x. However, we now
453 demonstrate that the PM1 is innervated only by retinula cell axons originating in the PME,
454 and connections between PM1 and AL1x seem to be absent. This coincides with Hill's (1975)
455 description for *Phidippus* spp., although he described additional neurites connecting PL1 and
456 PM1. It is likely that these neurites contribute to the tract that connects the first order visual
457 neuropils with the AB (compare Fig. 11a), instead of actually forming synapses in the PM1.
458 The PM1 differs from all other eyes by being connected to the AB only. Consequently, the
459 pathway of the PME lacks a second order visual neuropil. Information from this eye is not
460 processed within the mushroom bodies, but exclusively in the arcuate body.
461

462 **4.4 Second order visual neuropils of the ALE and PLE**

463 Visual neuropils with a glomerular structure have been found in the protocerebrum of several
464 spider species (e.g. Long, 2016). They have been termed "lame glomérulée" by Saint-Remy
465 (1887), "glomeruli" by Hanström (1921) and Babu & Barth (1984), "spherules" by Strausfeld
466 & Barth (1993) and "microglomeruli" by Steinhoff et al. (2017). The presence and
467 arrangement of these glomerular neuropils differs between spider species (Hanström, 1921;
468 Long, 2016) and some authors have considered them as a substructure of the MB (Babu and
469 Barth, 1984; Hill, 1975), whereas others have considered them to be separate second order
470 visual neuropils (Long, 2016; discussed in Steinhoff et al., 2017; Strausfeld and Barth, 1993).
471 Our results demonstrate, that in *M. muscosa*, the AL2/PL2 represents two closely adjoining
472 second order visual neuropils of the ALE and PLE, respectively. In *M. muscosa*, the AL2/PL2
473 was also found to react less plastically to different environmental conditions than the MBp
474 (Steinhoff et al., 2018), which was interpreted as further evidence for their function as
475 discrete visual neuropils. Within the AL2/PL2, each glomerulus seems to consist of numerous
476 synaptic complexes and Duelli (1980) estimated roughly 400 synapses per glomerulus in the
477 jumping spider *Evarcha arcuta*. Studies in insects used anti-synapsin labeling to detect
478 presynaptic sites, and phalloidin (which labels f-actin) to highlight postsynaptic sites of
479 synaptic complexes (Groh and Rössler, 2011). To investigate the AL2/PL2 of *M. muscosa*, we

480 have employed the same double-labeling approach (Fig. 9d-e), but the anti-synapsin and
481 phalloidin labeled areas in each synaptic complex were not clearly differentiated, as is the
482 case in social hymenopterans (Groh and Rössler, 2011), despite co-localization being minimal.
483 This might indicate that phalloidin does not consistently label postsynaptic sites in *M.*
484 *muscosa*, or that the organization of the pre- and postsynaptic sites within the AL2/PL2 of *M.*
485 *muscosa* differs compared to the glomeruli in mushroom body calyces of investigated insect
486 species. To clarify synaptic connectivity within the AL2/PL2 in *M. muscosa* and spiders in
487 general, a detailed transmission electron microscopic study is needed.
488

489 **4.5 Mushroom body pedunculus, haft and bridge**

490 The somata within SC2 of the neurons that connect the second order visual neuropils to the
491 MBp have been referred to as "globuli cells" (Hanström, 1921; Steinhoff et al., 2017) and the
492 neurons including these somata as "T-cells" (Strausfeld and Barth, 1993). In *C. salei*, globuli
493 cells have a smaller diameter of the soma and nucleus than other cell bodies in the
494 protocerebrum (Babu and Barth, 1984). We could not find such size differences in *M.*
495 *muscosa*. In fact, all three nuclear markers revealed that somata of the three identified
496 clusters as well the somata of the surrounding cortex exhibit a similar size (Figs. 2; 3; 5; 6; 7).
497 Thus, according to their definition (Kenyon, 1896; Richter et al., 2010), somata of SC2 are no
498 globuli cells in *M. muscosa*. The long neurites that connect the SC2 with the AL2/PL2 and the
499 L2 are probably primary neurites (Richter et al., 2010), from which dendrites branch into the
500 AL2/PL2 and L2 respectively, and axons project into the MBp, MBh and MBbr. A similar
501 arrangement has been described by Babu and Barth (1984) for *C. salei* and by Hill (1975) for
502 two *Phidippus* species.
503 The structure and organization of the MB differs between *M. muscosa* and *C. salei*, as already
504 reported by Steinhoff et al. (2017). The MBh is a separate structure of the mushroom body in
505 *M. muscosa,* connected to the MBp by neurites (Steinhoff et al., 2017), whereas in *C. salei*, it
506 is fused with the MBp (Strausfeld and Barth, 1993). Furthermore, the mushroom body shaft,
507 which in *C. salei* gives rise to the MBbr (Strausfeld and Barth, 1993) is absent or fused with
508 the MBp in *M. muscosa.*
509

510 **4.5 Functional considerations**

511 The jumping spider *Marpissa muscosa* and the wandering spider *Cupiennius salei* differ
512 strongly in their lifestyle. While *M. muscosa* is a diurnal hunter that actively pursues its prey

513 and relies on vision for prey capture, *C. salei* is an exclusively nocturnal sit-and-wait predator,
514 which detects its prey based on vibratory cues (Barth & Seyfarth, 1979). Although attack
515 behavior of *C. salei* can be elicited by visual cues under experimental conditions (Fenk et al.,
516 2010), mechanosensing is the major modality for hunting prey, since *C. salei* also captures
517 prey when its eyes are occluded (Hergenröder and Barth, 1983). Given these obvious
518 differences in lifestyle and relative importance of sensory modalities, it is surprising how
519 similar the general brain anatomy of *M. muscosa* and *C. salei* is. Apart from differences in size
520 and structure of neuropils, the visual pathway of the principal eyes is identical in *C. salei* and
521 *M. muscosa*. Parts of the visual pathways of the secondary eyes in the jumping spider
522 *Marpissa muscosa* differ, however, from those in the wandering spider *Cupiennius salei.*
523 These differences might reflect the differences in the visual fields and corresponding
524 functions of their secondary eyes (Land, 1985b; Land and Barth, 1992). The most conspicuous
525 difference between the visual systems in the brains of *M. muscosa* and *C. salei* is the pathway
526 of the PME. While the two larger secondary eyes (ALE and PLE) are connected to the
527 mushroom bodies in *M. muscosa,* the PME are not (Fig. 11). This suggests that the PME do
528 not play a role in motion detection (Duelli, 1978; Land, 1971; Zurek et al., 2010). In *C. salei,*
529 however, the PME are important movement detectors (Schmid, 1998) connected to the
530 mushroom bodies (Strausfeld and Barth, 1993).
531 Another interesting difference between the two species is the presence of the L2 in *M.*
532 *muscosa* (Steinhoff et al., 2017), which is absent in *C. salei*. The structure of this neuropil
533 differs from the AL2/PL2 and all second order visual neuropils in *C. salei,* since the L2 in *M.*
534 *muscosa* lacks a glomerular organization. Glomeruli might ensure a retinotopic organization
535 of neurites within the second order visual neuropils. This has been hypothesized for both *C.*
536 *salei* (Strausfeld and Barth, 1993) and for the PLE pathway of jumping spiders (Duelli, 1980),
537 where no lateral connections between individual glomeruli of the AL2/PL2 were found. We
538 hypothesize that while a retinotopic organization is kept in the AL2/PL2, it is lost in the L2.
539 Information from the movement-detecting ALE and PLE in *M. muscosa* might be integrated
540 not only in the MB, but also in the L2, and enable faster movement decisions. Alternatively, a
541 glomerular organization might be the most space-saving structure for the processing of input
542 from differentially tuned groups of axons (Eisthen, 2002; Hildebrand and Shepherd, 1997),
543 and although the L2 is not composed of glomeruli, information might still be processed in
544 parallel without lateral connections. This would also indicate that a higher number of neurites
545 synapse in the AL2/PL2 than in the L2 in *M. muscosa*.

Some early-branched off salticid species possess a large PME that has its own field of view (e.g. *Portia*; Land, 1985b; Maddison and Hedin, 2003). Land (1985b) suggested that in jumping spiders with a small PME, such as *M. muscosa*, the fields of view of ALE and PLE have expanded to fill the space not covered by the PME. The evolutionary transformation to a smaller PME and larger ALE and PLE might have led to visual pathways that also incorporated the L2. Thus in early-branched off jumping spiders with large PME, it could be hypothesized that the L2 might serve as a second order visual neuropil of the PME. Future studies should thus analyze the brain architecture of early-branched off salticid species.

CONFLICT OF INTEREST STATEMENT

The authors have no conflicts of interests.

AUTHOR CONTRIBUTIONS

All authors had full access to all the data in the study and take responsibility for the integrity of the data and the accuracy of data analysis. Study concept and design: POMS, AS, GU. Acquisition of data: POMS. Analysis and interpretation of data: POMS, AS. Wrote the manuscript: POMS, AS. Contributed to the writing of the manuscript: GU, SH. Obtained funding: GU, SH, POMS.

LITERATURE CITED

Babu, K.S., Barth, F.G., 1984. Neuroanatomy of the central nervous system of the wandering spider, *Cupiennius salei* (Arachnida, Araneida). Zoomorphology 104, 344–359. https://doi.org/10.1007/BF00312185

Barth, F., Seyfarth, E.-A., 1979. Cupiennius salei Keys. (Araneae) in the highlands of Central Guatemala. J. Arachnol. 7, 255–263.

Barth, F.G., 2002. The central nervous system, in: Barth, Friedrich G. (Ed.), A Spiders World; Senses and Behavior. Springer, Berlin Heidelberg, pp. 161–174.

Barth, F.G., Nakagawa, T., Eguchi, E., 1993. Vision in the ctenid spider *Cupiennius salei*: spectral range and absolute sensitivity. J. Exp. Biol. 79, 63–79. https://doi.org/ghjjagsj

Battelle, B.A., Calman, B.G., Andrews, A.W., Grieco, F.D., Mleziva, M.B., Callaway, J.C., Stuart, A.E., 1991. Histamine: A putative afferent neurotransmitter in *Limulus* eyes. J. Comp. Neurol. 305, 527–542. https://doi.org/10.1002/cne.903050402

Battelle, B.A., Sombke, A., Harzsch, S., 2016. Xiphosura, in: Schmidt-Rhaesa, A., Harzsch, Steffen, Purschke, G. (Eds.), Structure and Evolution of Invertebrate Nervous Systems. Oxford University Press, pp. 428–442.

580 Becherer, C., Schmid, A., 1999. Distribution of g-aminobutyric acid-, proctolin-, *Periplaneta*
581 hypertrehalosaemic hormone- and FMRFamide-like immunoreactivity in the visual
582 ganglia of the spider *Cupiennius salei* Keys. Comp. Biochem. Physiol. Part A 122, 267–
583 275.
584 Cebrià, F., 2008. Organization of the nervous system in the model planarian *Schmidtea*
585 *mediterranea*: An immunocytochemical study. Neurosci. Res. 61, 375–384.
586 https://doi.org/10.1016/j.neures.2008.04.005
587 Duelli, P., 1980. The neuronal organization of the posterior lateral eyes of jumping spiders
588 (Salticidae). Zool. Jahrbücher Abteilung für Anat. und Ontog. der Tiere 103, 17–40.
589 Duelli, P., 1978. Movement detection in the posterolateral eyes of jumping spiders (*Evarcha*
590 *arcuata*, Salticidae). J. Comp. Physiol. A 124, 15–26.
591 https://doi.org/10.1007/BF00656387
592 Eisthen, H.L., 2002. Why are olfactory systems of different animals so similar? Brain. Behav.
593 Evol. 59, 273–293. https://doi.org/10.1159/000063564
594 Fabian-Fine, R., Volknandt, W., Seyfarth, E.-A., 1999. Peripheral synapses at identifiable
595 mechanosensory neurons in the spider *Cupiennius salei*: synapsin-like
596 immunoreactivity. Cell Tissue Res. 295, 13–19.
597 Fenk, L.M., Hoinkes, T., Schmid, A., 2010. Vision as a third sensory modality to elicit attack
598 behavior in a nocturnal spider. J. Comp. Physiol. A 196, 957–961.
599 https://doi.org/10.1007/s00359-010-0575-8
600 Fenk, L.M., Schmid, A., 2010. The orientation-dependent visual spatial cut-off frequency in a
601 spider. J. Exp. Biol. 213, 3111–7. https://doi.org/10.1242/jeb.041939
602 Foelix, R.F., 1996. Biology of Spiders. Oxford University Press.
603 https://doi.org/10.2307/1535947
604 Garm, A., O'Connor, M., Parkefelt, L., Nilsson, D.-E., 2007. Visually guided obstacle
605 avoidance in the box jellyfish *Tripedalia cystophora* and *Chiropsella bronzie*. J. Exp. Biol.
606 210, 3616–3623. https://doi.org/10.1242/jeb.004044
607 Gregory, G.E., 1980. The bodian protargol technique, in: Strausfeld, N.J., Miller, T.A. (Eds.),
608 Neuroanatomical Techniques Insect Nervous System. Springer Berlin Heidelberg, pp.
609 75–95.
610 Groh, C., Rössler, W., 2011. Comparison of microglomerular structures in the mushroom
611 body calyx of neopteran insects. Arthropod Struct. Dev. 40, 358–367.
612 https://doi.org/10.1016/j.asd.2010.12.002

Hanström, B., 1921. Über die Histologie und vergleichende Anatomie der Sehganglien und Globuli der Araneen. K. Sven. Vetenskapsakademiens Handl. 61, 1–39.

Harland, D.P., Li, D., Jackson, R.R., 2012. How jumping spiders see the world, in: Lazareva, O.F., Shimizu, T., Wasserman, E.A. (Eds.), How Animals See the World: Comparative Behavior, Biology, and Evolution of Vision. Oxford University Press, pp. 133–164. https://doi.org/10.1093/acprof:oso/9780195334654.003.0010

Harzsch, S., Hansson, B.S., 2008. Brain architecture in the terrestrial hermit crab *Coenobita clypeatus* (Anomura, Coenobitidae), a crustacean with a good aerial sense of smell. BMC Neurosci. 9, 1–35. https://doi.org/10.1186/1471-2202-9-58

Harzsch, S., Müller, C.H., 2007. A new look at the ventral nerve centre of *Sagitta*: implications for the phylogenetic position of Chaetognatha (arrow worms) and the evolution of the bilaterian nervous system. Front. Zool. 4, 14.

Harzsch, S., Vilpoux, K., Blackburn, D.C., Platchetzki, D., Brown, N.L., Melzer, R., Kempler, K.E., Battelle, B.A., 2006. Evolution of arthropod visual systems: Development of the eyes and central visual pathways in the horseshoe crab *Limulus polyphemus* Linnaeus, 1758 (Chelicerata, Xiphosura). Dev. Dyn. 235, 2641–2655. https://doi.org/10.1002/dvdy.20866

Harzsch, S., Wildt, M., Battelle, B., Waloszek, D., 2005. Immunohistochemical localization of neurotransmitters in the nervous system of larval *Limulus polyphemus* (Chelicerata, Xiphosura): Evidence for a conserved protocerebral architecture in Euarthropoda. Arthropod Struct. Dev. 34, 327–342. https://doi.org/10.1016/j.asd.2005.01.006

Hergenröder, R., Barth, F.G., 1983. Vibratory signals and spider behavior: How do the sensory inputs from the eight legs interact in orientation? J. Comp. Physiol. A 152, 361–371. https://doi.org/10.1007/BF00606241

Hildebrand, J.G., Shepherd, G.M., 1997. Mechanisms of olfactory discrimination: Converging evidence for common principles across phyla. Annu. Rev. Neurosci. 20, 595–631. https://doi.org/10.1146/annurev.neuro.20.1.595

Hill, D.E., 1975. The structure of the central nervous system of jumping spiders of the genus *Phidippus* (Araneae: Salticidae). M.Sc. thesis; Oregon State University.

Homann, H., 1952. Die Nebenaugen der Araneen. Zweite Mitteilung. Zoologische Jahrbücher Abteilung für Anatomie und Ontogenie der Tiere 72, 345–364.

Homann, H., 1950. Die Nebenaugen der Araneen. Zoologische Jahrbücher Abteilung für Anatomie und Ontogenie der Tiere 71, 56–144.

646 Jakob, E.M., Long, S.M., Harland, D.P., Jackson, R.R., Carey, A., Searles, M.E., Porter, A.H.,
647 Canavesi, C., Rolland, J.P., 2018. Lateral eyes direct principal eyes as jumping spiders
648 track objects. Curr. Biol. 28, R1092–R1093. https://doi.org/10.1016/j.cub.2018.07.065
649 Kenyon, F.C., 1896. The meaning and structure of the so-called "mushroom bodies" of the
650 hexapod brain. Am. Nat. 643–650.
651 Klagges, B.R.E., Heimbeck, G., Godenschwege, T.A., Hofbauer, A., Pflugfelder, G.O.,
652 Reifegerste, R., Reisch, D., Schaupp, M., Buchner, S., Buchner, E., 1996. Invertebrate
653 synapsins: a single gene codes for several isoforms in *Drosophila*. J. Neurosci. 16, 3145–
654 3165.
655 Land, M.F., 1985a. The morphology and optics of spider eyes, in: Barth, F.G. (Ed.),
656 Neurobiology of Arachnids. Springer, Berlin, pp. 53–76. https://doi.org/10.1007/978-3-
657 642-70348-5_4
658 Land, M.F., 1985b. Fields of view of the eyes of primitive jumping spiders. J. Exp. Biol. 119,
659 381–384.
660 Land, M.F., 1972. Mechanisms of orientation and pattern recognition by jumping spiders
661 (Salticidae), in: Wehner, R. (Ed.), Information Processing in the Visual Systems of
662 Anthropods. Springer Berlin Heidelberg, pp. 231–247.
663 Land, M.F., 1971. Orientation by jumping spiders in the absence of visual feedback. J. Exp.
664 Biol. 54, 119–139.
665 Land, M.F., Barth, F.G., 1992. The quality of vision in the ctenid spider *Cupiennius salei*. J.
666 Exp. Biol. 164, 227–242.
667 Lehmann, T., Melzer, R.R., 2018. Also looking like *Limulus*? - retinula axons and visual
668 neuropils of Amblypygi (whip spiders). Front. Zool. 15, 52.
669 https://doi.org/10.1186/s12983-018-0293-6
670 Lehmann, T., Melzer, R.R., 2013. Looking like *Limulus*? - Retinula axons and visual neuropils
671 of the median and lateral eyes of scorpions. Front. Zool. 10, 40.
672 https://doi.org/10.1186/1742-9994-10-40
673 Lehmann, T., Melzer, R.R., Hörnig, M.K., Michalik, P., Sombke, A., Harzsch, S., 2016.
674 Arachnida (excluding scorpiones), in: Schmidt-Rhaesa, A., Harzsch, S., Purschke, G.
675 (Eds.), Structure and Evolution of Invertebrate Nervous Systems. Oxford University
676 Press, Oxford, pp. 453–477.
677 Loesel, R., Wolf, H., Kenning, M., Harzsch, S., Sombke, A., 2013. Architectural principles and
678 evolution of the arthropod central nervous system, in: Minelli, A. (Ed.), Arthropod

Biology and Evolution. Springer-Verlag, Berlin Heidelberg, pp. 299–342. https://doi.org/10.1007/978-3-642-36160-9

Long, S.M., 2016. Spider Brain Morphology & Behavior. PhD thesis; University of Massachusetts, Amherst.

Maddison, W.P., Hedin, M.C., 2003. Jumping spider phylogeny (Araneae: Salticidae). Invertebr. Syst. 17, 529. https://doi.org/10.1071/is02044

Morehouse, N.I., Buschbeck, E.K., Zurek, D.B., Steck, M., Porter, M.L., 2017. Molecular evolution of spider vision: New opportunities, familiar players. Biol. Bull. 233, 21–38. https://doi.org/10.1086/693977

Nagata, T., Arikawa, K., Kinoshita, M., 2019. Photoreceptor projection from a four-tiered retina to four distinct regions of the first optic ganglion in a jumping spider. J. Comp. Neurol. 1–14. https://doi.org/10.1002/cne.24584

Nässel, D.R., 1999. Histamine in the brain of insects: a review. Microsc. Res. Tech. 44, 121–136. https://doi.org/10.1002/(SICI)1097-0029(19990115/01)44:2/3<121::AID-JEMT6>3.0.CO;2-F

O'Connor, M., Garm, A., Nilsson, D.E., 2009. Structure and optics of the eyes of the box jellyfish *Chiropsella bronzie*. J. Comp. Physiol. A 195, 557–569. https://doi.org/10.1007/s00359-009-0431-x

Orlando, E., Schmid, A., 2011. Colour blindness of the movement-detecting system of the spider *Cupiennius salei*. J. Exp. Biol. 214, 546–550. https://doi.org/10.1242/jeb.051672

Ott, S.R., 2008. Confocal microscopy in large insect brains: Zinc-formaldehyde fixation improves synapsin immunostaining and preservation of morphology in whole-mounts. J. Neurosci. Methods 172, 220–230. https://doi.org/10.1016/j.jneumeth.2008.04.031

Paulus, H., 1979. Eye structure and the monophyly of the Arthropoda, in: AP, G. (Ed.), Arthropod Phylogeny. Vam Nostrand Reinhold Company, New York., pp. 299-383.

Richter, S., Loesel, R., Purschke, G., Schmidt-Rhaesa, A., Scholtz, G., Stach, T., Vogt, L., Wanninger, A., Brenneis, G., Döring, C., Faller, S., Fritsch, M., Grobe, P., Heuer, C.M., Kaul, S., Møller, O.S., Müller, C.H., Rieger, V., Rothe, B.H., Stegner, M.E., Harzsch, S., 2010. Invertebrate neurophylogeny: suggested terms and definitions for a neuroanatomical glossary. Front. Zool. 7, 29. https://doi.org/10.1186/1742-9994-7-29

Saint Rémy, G., 1887. Contribution à l'étude du cerveau chez les Arthropodes trachéates. Arch. Zool. Exp. Générale.

Schmid, A., 1998. Different functions of different eye types in the spider *Cupiennius salei*. J.

712 Exp. Biol. 201, 221–5.
713 Schmid, A., Duncker, M., 1993. Histamine immunoreactivity in the central nervous system of
714 the spider *Cupiennius salei*. Cell Tissue Res. 273, 533–545.
715 https://doi.org/10.1007/BF00333707
716 Schulze, E., Graupner, H., 1960. Anleitung zum mikroskopisch-technischen Arbeiten in
717 Biologie und Medizin. Akademische Verlagsgesellschaft.
718 Sombke, A., Harzsch, S., 2015. Immunolocalization of histamine in the optic neuropils of
719 *Scutigera coleoptrata* (Myriapoda: Chilopoda) reveals the basal organization of visual
720 systems in Mandibulata. Neurosci. Lett. 594, 111–6.
721 https://doi.org/10.1016/j.neulet.2015.03.029
722 Sombke, A., Harzsch, S., Hansson, B.S., 2011. Organization of deutocerebral neuropils and
723 olfactory behavior in the centipede *Scutigera coleoptrata* (Linnaeus, 1758) (Myriapoda:
724 Chilopoda). Chem. Senses 36, 43–61. https://doi.org/10.1093/chemse/bjq096
725 Sombke, A., Lipke, E., Michalik, P., Uhl, G., Harzsch, S., 2015. Potential and limitations of x-
726 ray micro-computed tomography in arthropod neuroanatomy: a methodological and
727 comparative survey. J. Comp. Neurol. 523, 1281–1295.
728 https://doi.org/10.1002/cne.23741
729 Spano, L., Long, S.M., Jakob, E.M., 2012. Secondary eyes mediate the response to looming
730 objects in jumping spiders (*Phidippus audax*, Salticidae). Biol. Lett. 8, 949–951.
731 https://doi.org/10.1098/rsbl.2012.0716
732 Steinhoff, P.O.M., Liedtke, J., Sombke, A., Schneider, J.M., Uhl, G., 2018. Early environmental
733 conditions affect the volume of higher-order brain centers in a jumping spider. J. Zool.
734 304, 182–192. https://doi.org/10.1111/jzo.12512
735 Steinhoff, P.O.M., Sombke, A., Liedtke, J., Schneider, J.M., Harzsch, S., Uhl, G., 2017. The
736 synganglion of the jumping spider *Marpissa muscosa* (Arachnida: Salticidae): Insights
737 from histology, immunohistochemistry and microCT analysis. Arthropod Struct. Dev.
738 46, 156–170. https://doi.org/10.1016/j.asd.2016.11.003
739 Strausfeld, N.J., 2012. Arthropod Brains: Evolution, Functional Elegance, and Historical
740 Significance, Cambridge: Harvard UP. Belknap Press of Harvard University Press,
741 Cambridge.
742 Strausfeld, N.J., Barth, F.G., 1993. Two visual systems in one brain: Neuropils serving the
743 secondary eyes of the spider *Cupiennius salei*. J. Comp. Neurol. 328, 43–62.
744 https://doi.org/10.1002/cne.903280105

745 Strausfeld, N.J., Weltzien, P., Barth, F.G., 1993. Two visual systems in one brain: Neuropils
746 serving the principal eyes of the spider *Cupiennius salei*. J. Comp. Neurol. 328, 63–75.
747 https://doi.org/10.1002/cne.903280105
748 Sullivan, J.M., Benton, J.L., Sandeman, D.C., Beltz, B.S., 2007. Adult neurogenesis: A common
749 strategy across diverse species. J. Comp. Neurol. 500, 574–584.
750 https://doi.org/10.1002/cne.21187
751 Weltzien, P., Barth, F.G., 1991. Volumetric measurements do not demonstrate that the
752 spider brain "central body" has a special role in web building. J. Morphol. 208, 91–98.
753 https://doi.org/10.1002/jmor.1052080104
754 Widmer, A., Höger, U., Meisner, S., French, A.S., Torkkeli, P.H., 2005. Spider peripheral
755 mechanosensory neurons are directly innervated and modulated by octopaminergic
756 efferents. J. Neurosci. 25, 1588–1598. https://doi.org/10.1523/jneurosci.4505-04.2005
757 Yamashita, S., Tateda, H., 1978. Spectral sensitivities of the anterior median eyes of the orb
758 web spiders, *Argiope bruennichii* and *A. amoena*. J. Exp. Biol. 74, 47–57.
759 Yamashita, S., Tateda, H., 1976. Spectral sensitivities of jumping spider eyes. J. Comp.
760 Physiol. A 105, 29–41. https://doi.org/10.1007/BF01380051
761 Zurek, D.B., Nelson, X.J., 2012a. Hyperacute motion detection by the lateral eyes of jumping
762 spiders. Vision Res. 66, 26–30. https://doi.org/10.1016/j.visres.2012.06.011
763 Zurek, D.B., Nelson, X.J., 2012b. Saccadic tracking of targets mediated by the anterior-lateral
764 eyes of jumping spiders. J. Comp. Physiol. A 198, 411–417.
765 https://doi.org/10.1007/s00359-012-0719-0
766 Zurek, D.B., Taylor, A.J., Evans, C.S., Nelson, X.J., 2010. The role of the anterior lateral eyes in
767 the vision-based behaviour of jumping spiders. J. Exp. Biol. 213, 2372–8.
768 https://doi.org/10.1242/jeb.042382
769
770
771
772
773
774
775 **Tables**
776 **Table 1** Primary and secondary antibodies

Labeling reagent	Dilution and specifications
Primary	

Monoclonal anti-synapsin antibody produced in mouse (RRID AB_528479)	1:1000, DSHB 3C11 Steinhoff et al. (2017), this study
Polyclonal anti α-tubulin antibody produced in rabbit (RRID AB_2637882)	1:1000 or 1:250, ThermoFisher PA5-58711
Monoclonal anti-acetylated α-tubulin antibody produced in mouse (RRID AB_477585)	1:1000, Sigma Aldrich T6793
Monoclonal anti-histamine antibody produced in rabbit (RRID AB_1541510)	1:1000, Progen 16043 Harzsch et al. (2005), Sombke and Harzsch (2015)
Secondary	
Polyclonal Cy3 anti-mouse IgG secondary anti- body produced in goat (RRID AB_2338680)	1:500, Jackson Immuno Research, 115–165-003
Polyclonal Alexa 488 anti-rabbit IgG secondary antibody produced in goat (RRID AB_2534074)	1:500, Invitrogen, A11006
Alexa Fluor 488 phalloidin (RRID AB_2315147)	1:50, Molecular Probes A-12379
Hoechst 33258	1:1000, Sigma 14530
YOYO 1 491	Molecular Probes Y-3601

Table 2 Methods and antisera combinations

Methods	Antisera combinations/ staining	Coupled with	Specimens
Wholemount	anti-synapsin	Cy3 anti-mouse (goat)	5
Vibratome sections (50 µm; 80 µm)	anti-synapsin (mouse) anti- α-tubulin (rabbit)	Cy3 anti-mouse (goat) Alexa Fluor 488 anti-rabbit (goat) Nuclear labeling: Hoechst 33258	16
	anti-acetylated-α-tubulin (mouse)	Nuclear labeling: YOYO	6
	anti-histamine (rabbit)	Alexa Fluor 488 anti-rabbit (goat)	4
	anti-synapsin (mouse)	Cy3 anti-mouse (goat) Phalloidin	5
Paraffin sections (5 µm)	Azan-novum	/	2
microCT scans	1% idodine (in 99% ethanol)	/	4

Figures

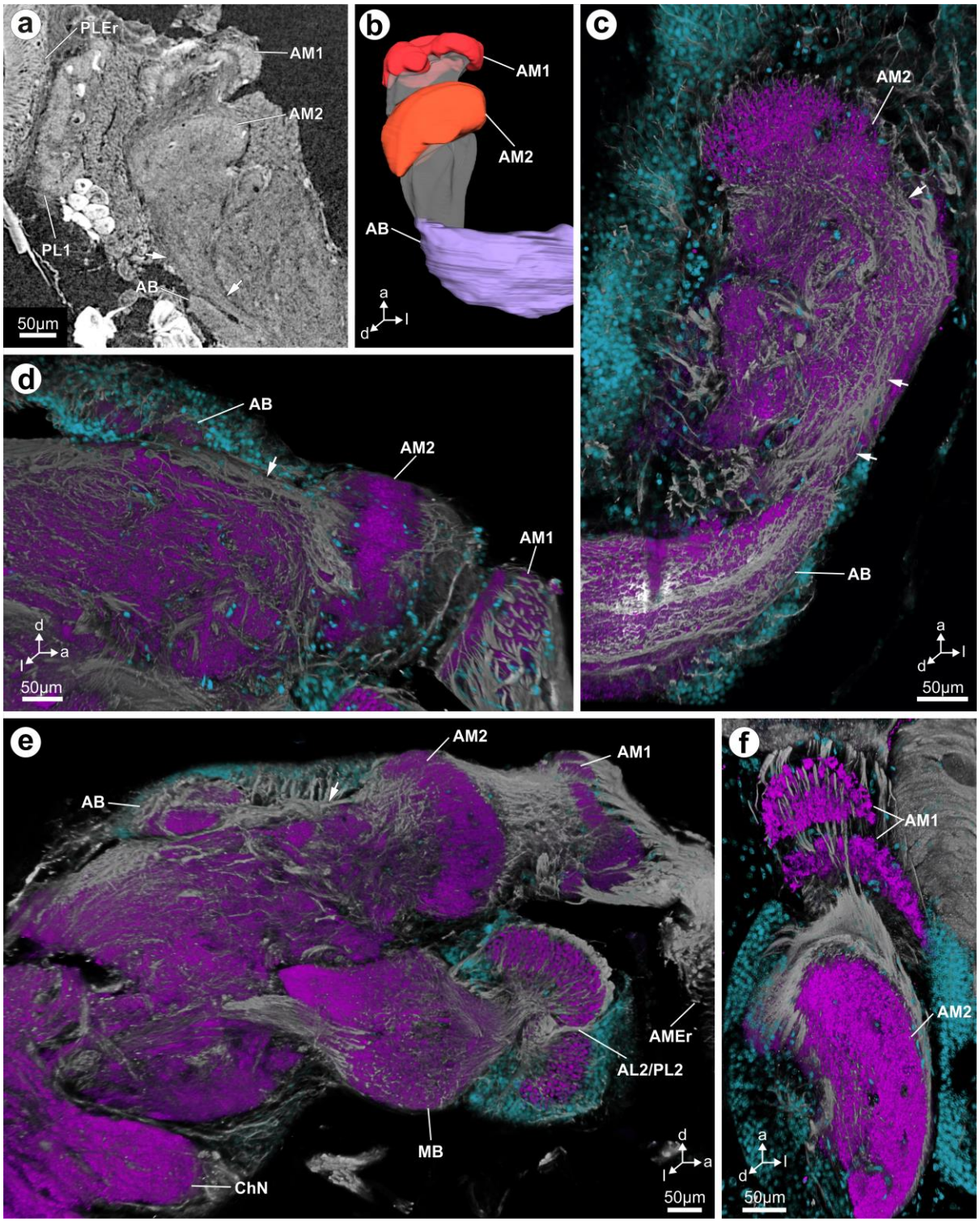

Figure 1. The principal eye pathway in *Marpissa muscosa*. **a** Virtual horizontal section of the dorsal protocerebrum obtained by microCT analysis shows the connections between the AM1, AM2 and the AB. **b** Three-dimensional reconstruction based on a microCT image stack shows the same connections as in a. **c-f** Maximum projection of image stacks (clsm), show tubulin-immunoreactivity (grey) and somata (blue) in the protocerebrum of *Marpissa muscosa*. **c** Horizontal section showing the AM2, the AB and connecting neurites (arrows). **d**

Sagittal section through the AM1, AM2 and the AB showing the connecting neurites between AM2 and AB (arrow). **e** Sagittal section showing at least two lobes of the AM1, the thick tract to the AM2 and the thinner connection to the AB (arrow). AL2/PL2 and MB are also visible. **f** Horizontal section showing two lobes of the AM1, retinula cell axons terminating in those and interneurons connecting AM1 with AM2. **Abbreviations: a** anterior, **AB** arcuate body, **AL2/PL2** second order visual neuropil of anterior lateral and posterior lateral eyes, **AM1** first order visual neuropil of the anterior median eyes, **AM2** second order visual neuropil of the anterior median eyes, **AMEr** retina of the anterior median eyes, **ChN** cheliceral neuropil, **d** dorsal, **l** lateral, **MB** mushroom body, **PL1** first order visual neuropil of the posterior lateral eyes, **PLEr** retina of the posterior lateral eyes, **PM1** first order visual neuropil of the posterior median eyes.

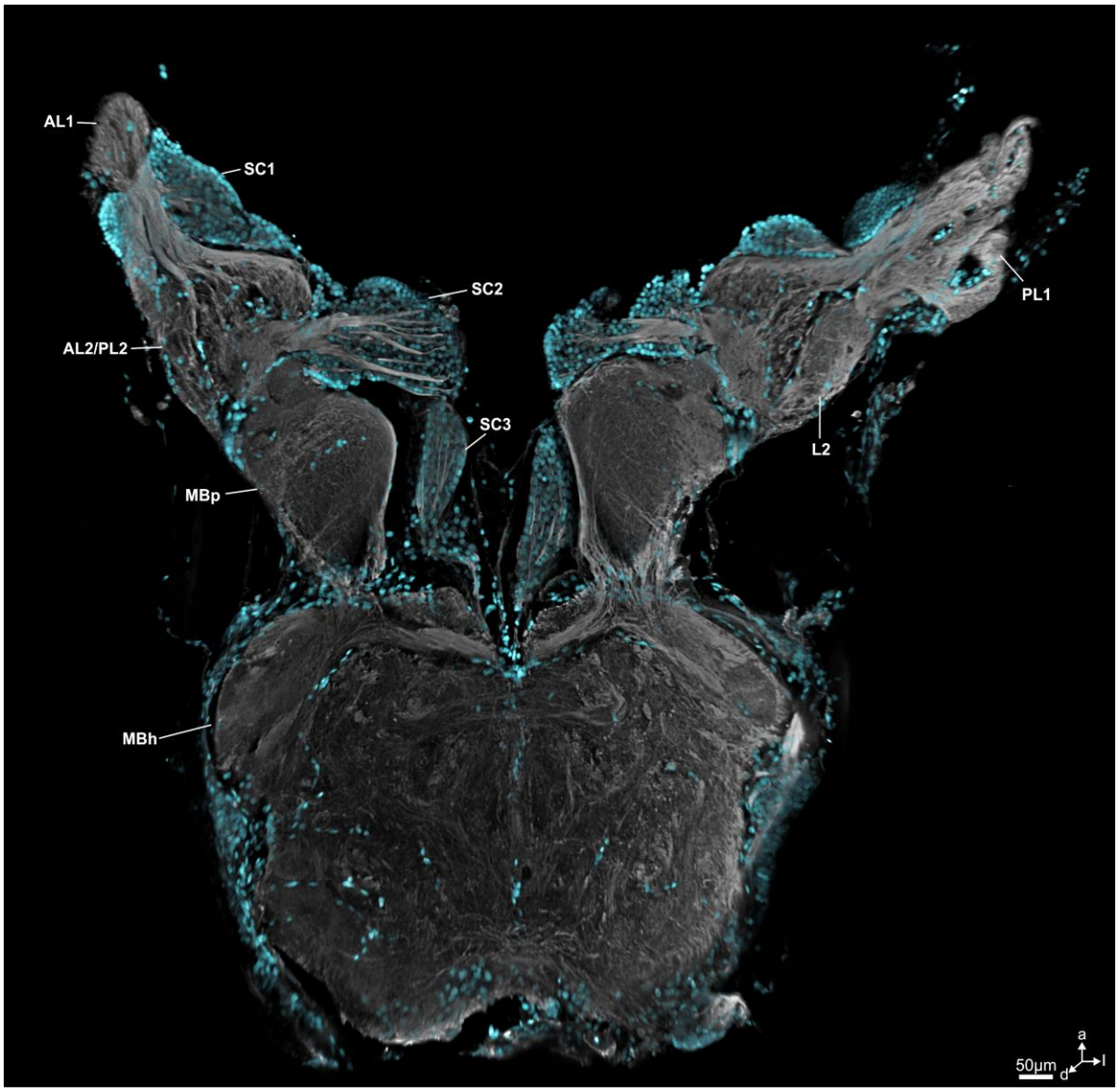

Figure 2. Maximum projection of an image stack (clsm), showing tubulin-immunoreactivity (grey) and somata (blue) in the protocerebrum of *Marpissa muscosa*. The AL1 and PL1 are connected to both, the AL2/PL2 and the L2. The neurites forming these connections originate in SC1. The AL2/PL2 and the L2 are connected to the MBp via neurites, which originate in the SC2. The two MBp are connected with each other via the mushroom body bridge, which is formed by long neurites that project along the periphery of the MBp and seem to originate in the SC2. Some of these long neurites also connect the MBp with the MBh. Other neurites originate in SC3 and enter the protocerebrum medially. **Abbreviations: a** anterior, **AL1** first order visual neuropil of the anterior lateral eyes, **AL2/PL2** second order visual neuropil of ALE and PLE, **d** dorsal, **l** lateral, **L2** shared second order visual neuropil of the anterior lateral and posterior lateral eyes, **MBh** mushroom body haft, **MBp** mushroom body pedunculus, **SC1-3** soma cluster 1-3.

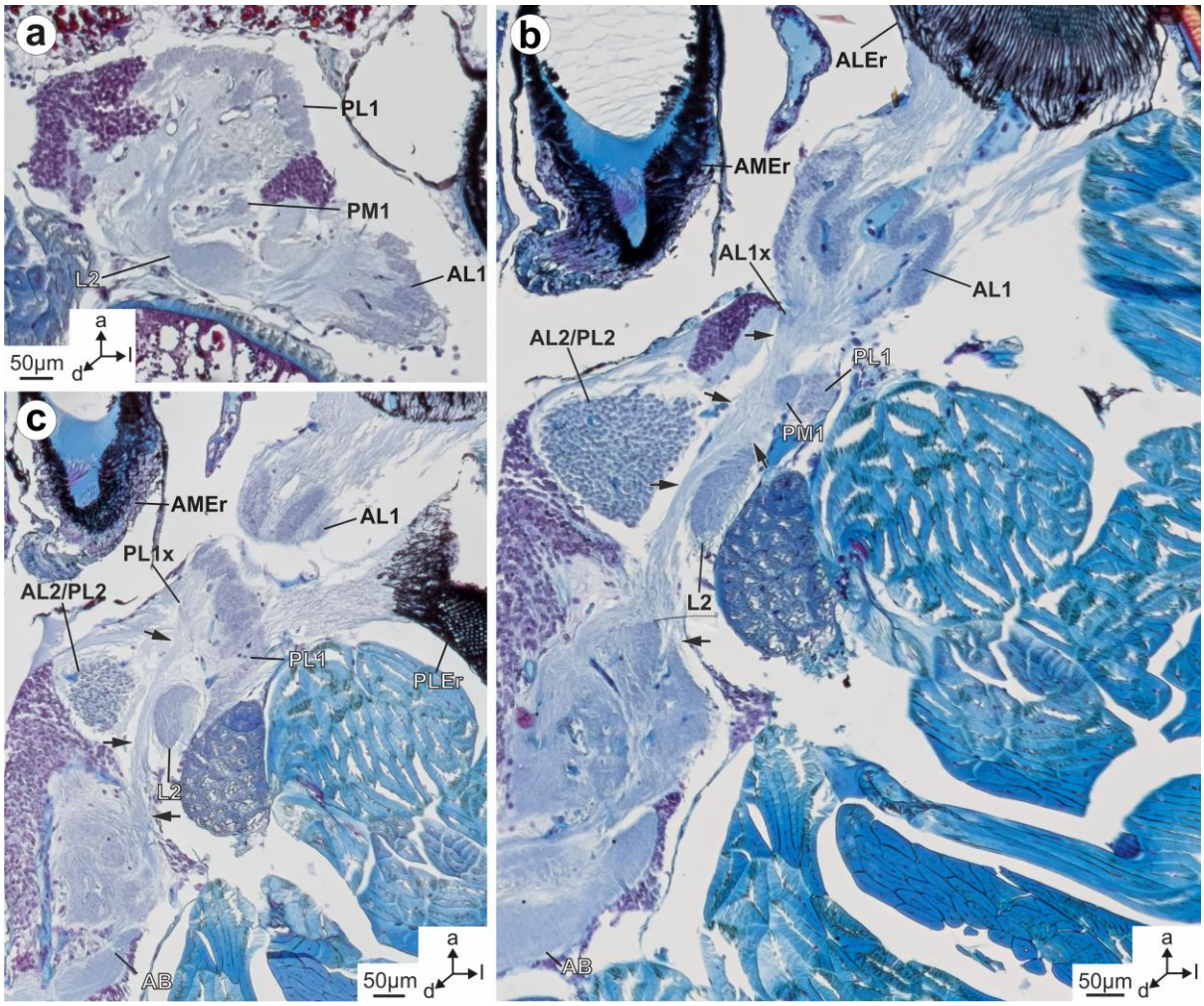

Figure 3. Paraffin sections through the anterior protocerebrum of *Marpissa muscosa.* **a** Sagittal section showing the conspicuous tracts that connect the AL1 and PL1 with the L2. **b** Horizontal section showing the convoluted and columnar structure of the AL1. Neurites that connect the AL1 with the AB probably synapse in the AL1x. Long neurites connecting the PL1 with the AB are visible curving around L2. Other long neurites contributing to the tract to the AB synapse in PM1. Arrows point to neurites contributing to the tract between first order visual neuropils of the secondary eyes and the arcuate body. **c** Horizontal section showing several neurites that connect the PL1 with the AL2/PL2, as well as the neurites contributing to the tract between the PL1 and the AB (highlighted by arrows). **Abbreviations: a** anterior, **AB** arcuate body, **AL1** first order visual neuropil of the anterior lateral eyes, **AL1x** neuropilar subunit of the AL1, **AL2/PL2** second order visual neuropil of anterior lateral and posterior lateral eyes, **ALEr** retina of the anterior lateral eyes, **AMEr** retina of the anterior median eyes, **d** dorsal, **l** lateral, **L2** shared second order visual neuropil of the anterior lateral and posterior lateral eyes, **PL1** first order visual neuropil of the posterior lateral eyes, **PLEr** retina of the anterior lateral eyes, **PL1x** neuropilar subunit of the PL1, **PM1** first order visual neuropil of the posterior median eyes**.**

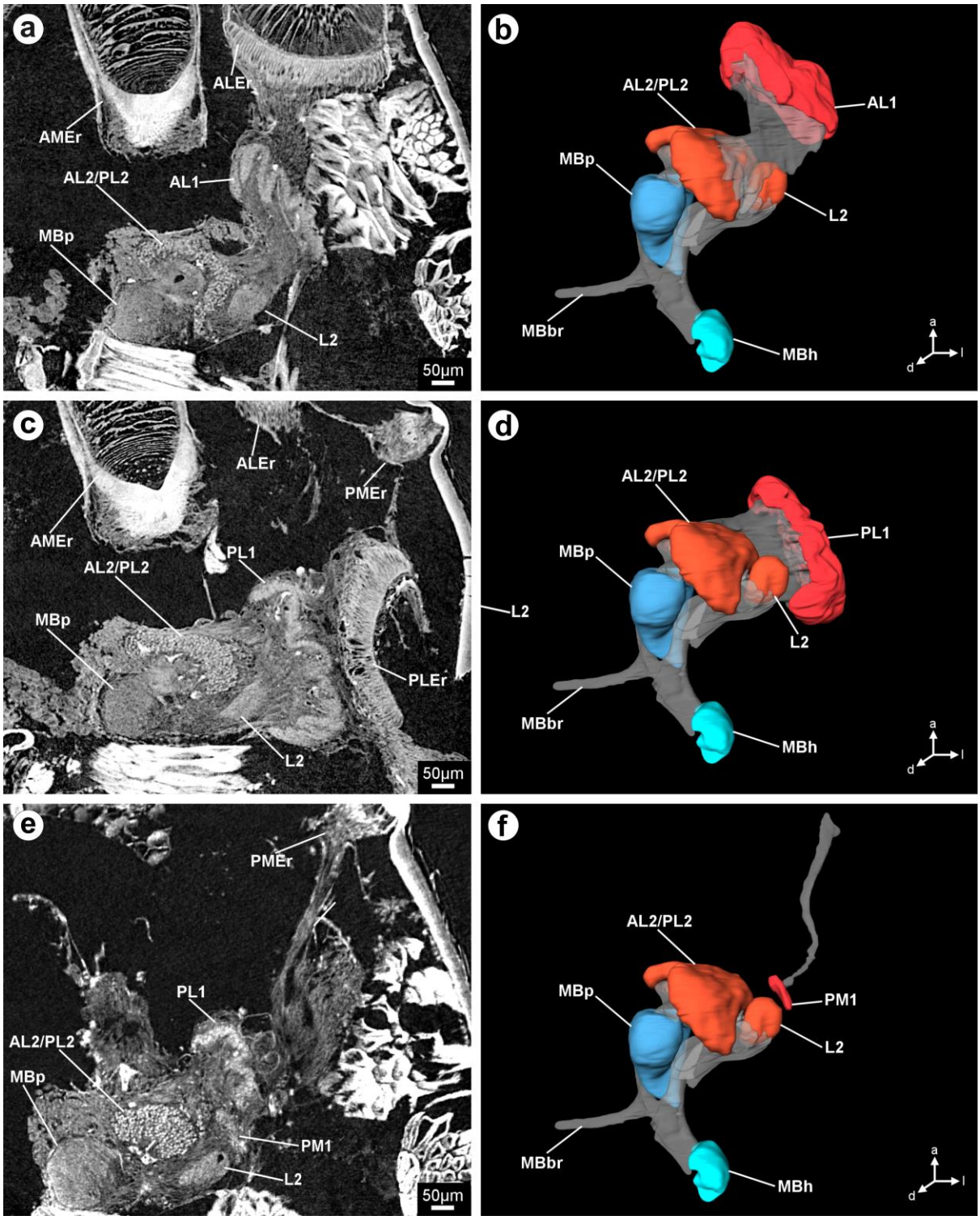

Figure 4. Protocerebral neuropils depicted in different virtual horizontal sections obtained by microCT analysis (**a, c, e**) and three-dimensional reconstructions based on microCT image stacks (**b, d, f**). **a** + **b** The retina of the ALE is located very closely to its first order visual neuropil, the AL1. The AL1 has a convoluted surface and is connected to the AL2/PL2 and the L2. **c** + **d** The retina of the PLE almost comes in contact with its first order visual neuropil, the PL1. The PL1 has a convoluted surface and is connected to the MB and the L2. **e** + **f** A comparatively long optic nerve connects the retina of the PME with its first order visual

neuropil, the PM1. See supporting information for an interactive 3D-visualization of the microCT reconstruction. **Abbreviations: a** anterior, **AL1** first order visual neuropil of the anterior lateral eyes, **AL2/PL2** second order visual neuropil of anterior lateral and posterior lateral eyes, **ALEr** retina of the anterior lateral eyes, **AMEr** retina of the anterior median eyes, **d** dorsal, **l** lateral, **L2** shared second order visual neuropil of the anterior lateral and posterior lateral eyes, **MBbr** mushroom body bridge, **MBh** mushroom body haft, **MBp** mushroom body pedunculus, **PL1** first order visual neuropil of the posterior lateral eyes, **PLEr** retina of the posterior lateral eyes, **PM1** first order visual neuropil of the posterior median eyes, **PMEr** retina of the posterior median eyes.

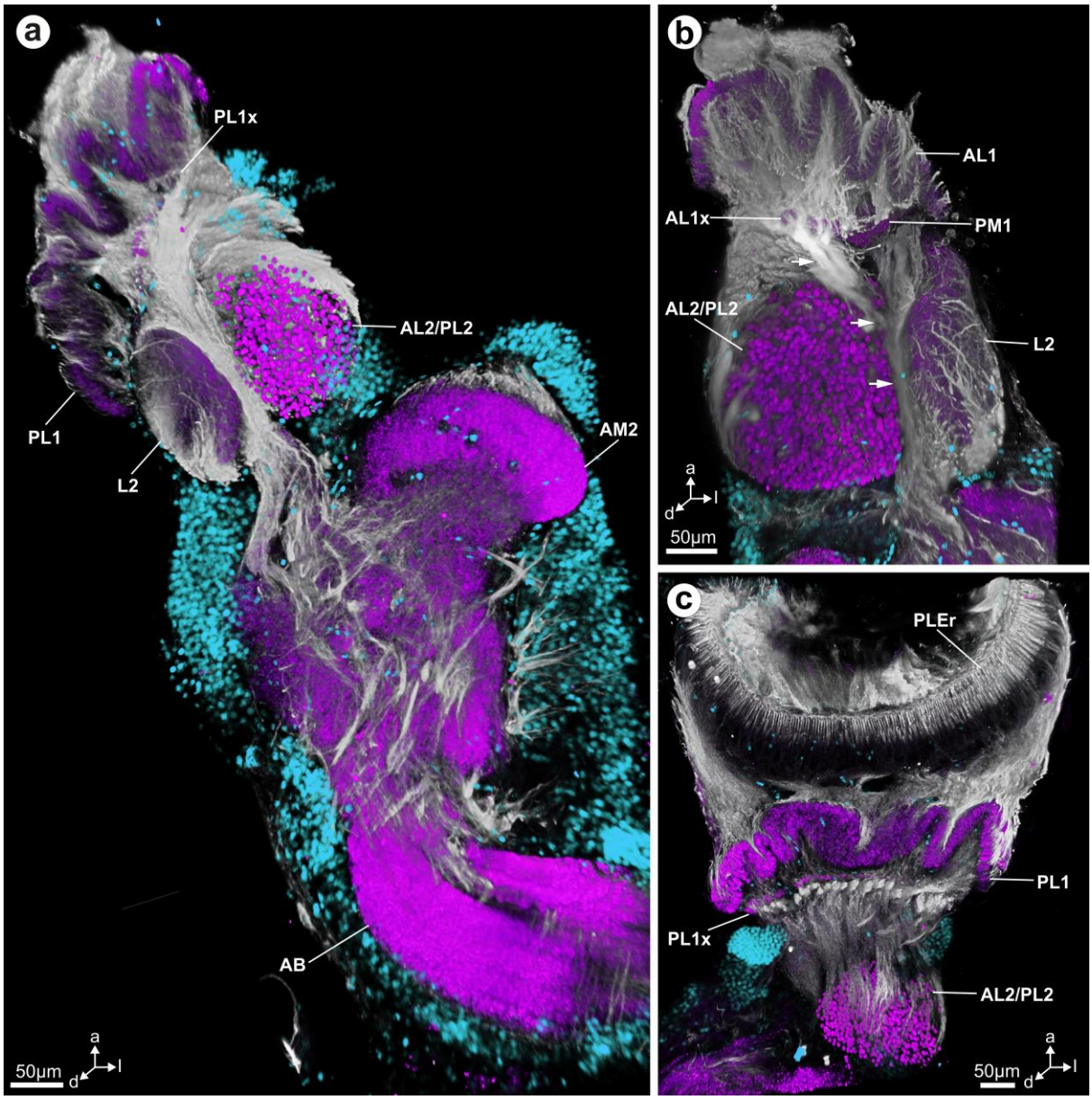

Figure 5. Maximum projections of image stacks (clsm) showing tubulin-immunoreactivity (grey), synapsin-immunoreactivity (magenta) and somata (blue) in the secondary eye visual pathway of *Marpissa muscosa*. **a** Neurites from the PL1 pass between AL2/PL2 and L2 towards the AB. **b** Neurites from AL1x join the tract from the PM1 that passes through between AL2/PL2 and L2 (highlighted by arrows). **c** The PL1 is in close spatial relationship to the PLEr. Parallel neurites connect the PL1 and PL1x with the Al2/PL2. **Abbreviations: a** anterior, **AB** arcuate body, **AL1** first order visual neuropil of the anterior lateral eyes, **AL1x** neuropilar subunit of the AL1, **AL2/PL2** second order visual neuropil of anterior lateral and posterior lateral eyes, **AM2** second order visual neuropil of the anterior median eyes, **d** dorsal, **l** lateral, **L2** shared second order visual neuropil of the anterior lateral and posterior lateral eyes, **MBp** mushroom body pedunculus, **PL1** first order visual neuropil of the posterior lateral eyes, **PL1x**

neuropilar subunit of the PL1, **PLEr** retina of the posterior lateral eyes, **PM1** first order visual neuropil of the posterior median eyes.

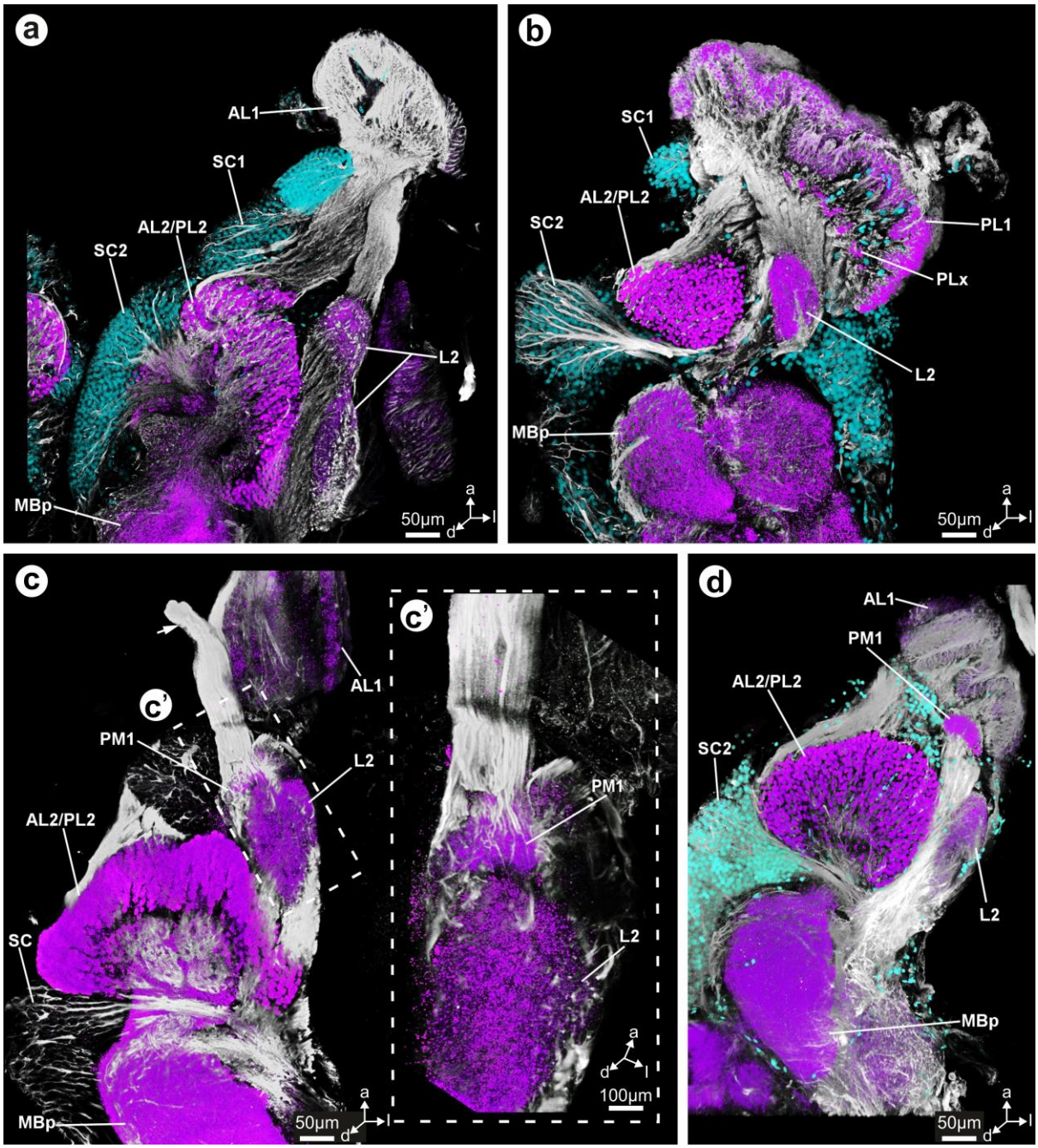

Figure 6. Maximum projections of image stacks (clsm) showing tubulin-immunoreactivity (grey), synapsin-immunoreactivity (magenta) and somata (blue) in the secondary eye visual pathway of *Marpissa muscosa*. **a** The AL1 is connected to the AL2/PL2 and the L2 via two prominent neurite tracts. Some of the neurites contributing to these tracts originate in SC1. Neurites connecting the AL2/PL2 with the MBp originate in SC2. **b** The PL1 is connected to the AL2/PL2 and the L2 via two prominent neurite tracts. Some neurites that arise in SC2 pass between AL2/PL2 and MBp towards the L2. **c** The optic nerve of the PME (highlighted by arrow) terminates in the PM1. **c'** Higher magnification of C, showing the termination site of the PME optic nerve in the PM1. **d** Neurites from the PM1 pass between AL2/PL2 and L2. **Abbreviations: a** anterior, **AL1** first order visual neuropil of the anterior lateral eyes, **AL2/PL2**

second order visual neuropil of anterior lateral and posterior lateral eyes, **d** dorsal, **l** lateral, **L2** shared second order visual neuropil of the anterior lateral and posterior lateral eyes, **MBp** mushroom body pedunculus, **PL1** first order visual neuropil of the posterior lateral eyes, **PL1x** neuropilar subunit of the PL1, **PM1** first order visual neuropil of the posterior median eyes, **SC1-2** soma cluster 1-2.

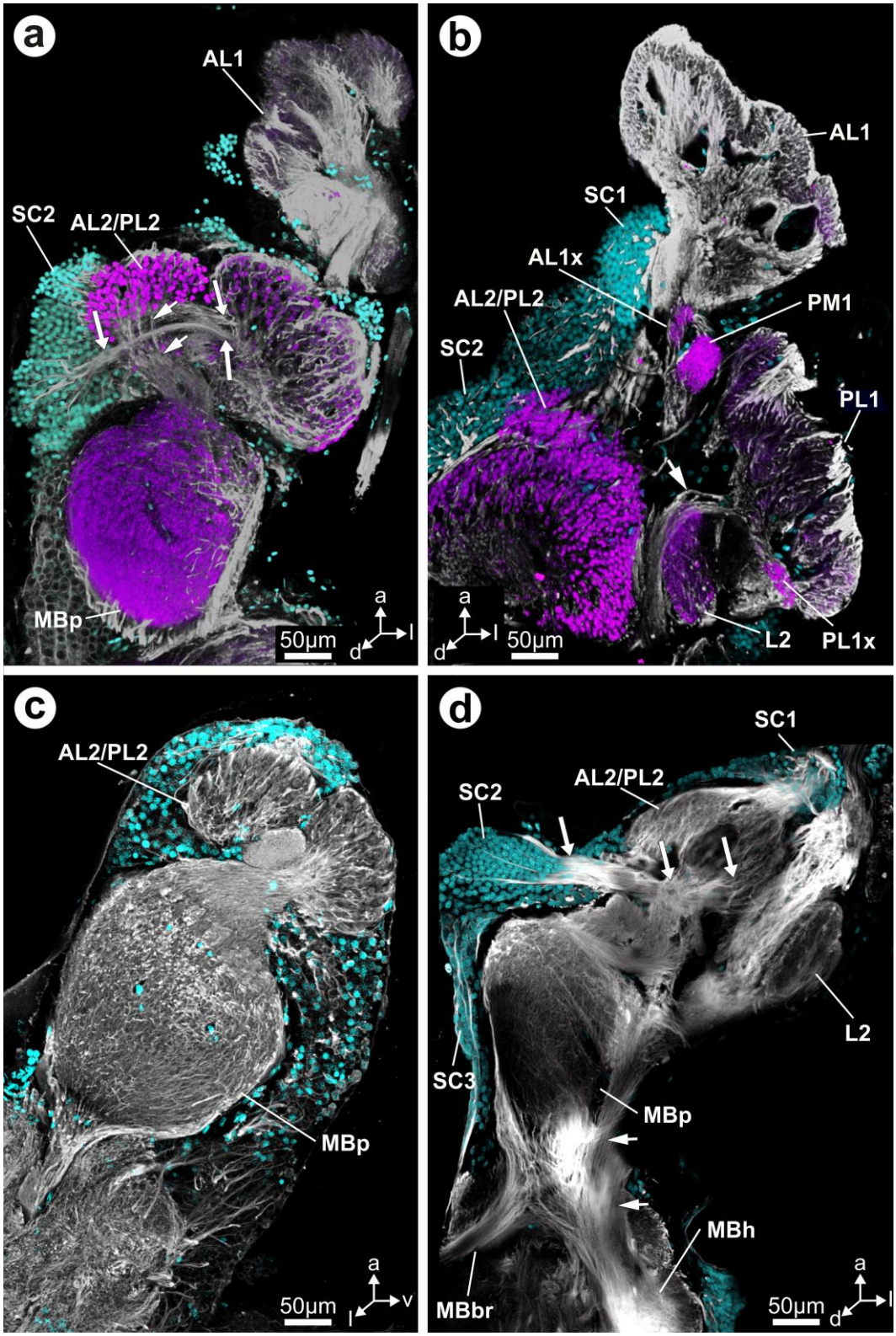

Figure 7. Maximum projections of image stacks (clsm) showing tubulin-immunoreactivity (grey), synapsin-immunoreactivity (magenta) and somata (blue) in the secondary eye visual pathway of *Marpissa muscosa*. **a** Horizontal section through AL1, MBp and AL2/PL2. The AL1 connects to one of the two tightly adjoining clusters of AL2/PL2. Arrows point to primary neurites connecting SC2 and AL2/PL2. Arrowheads point to neurites connecting the AL2/PL2 with the MBp. **b** Horizontal section through visual neuropils. The PM1 is situated between

AL1 and PL1, AL2/PL2 appear as a uniform array. The arrowhead points to neurites connecting PL1 with AB, neurites probably synapse in the PL1x. **c** A sagittal section through AL2/PL2 and MBp reveals two distinct clusters of AL2/PL2 and the chiasm formed by neurites that connect AL2/PL2 with MBp. **d** Tubulin-immunoreactivity shows long peripheral neurites contributing to the MBbr and connecting the MBp with the MBh. Arrows point to primary neurites connecting SC2 with the AL2/PL2. Arrowheads point to neurites connecting the MBp with the MBh. **Abbreviations: a** anterior, **AL1** first order visual neuropil of the anterior lateral eyes, **AL1x** neuropilar subunit of the AL1, **AL2/PL2** second order visual neuropil of anterior lateral and posterior lateral eyes, **d** dorsal, **l** lateral, **L2** shared second order visual neuropil of the anterior lateral and posterior lateral eyes, **MBbr** mushroom body bridge, **MBh** mushroom body haft, **MBp** mushroom body pedunculus, **PL1** first order visual neuropil of the posterior lateral eyes, **PL1x** neuropilar subunit of the PL1, **PM1** first order visual neuropil of the posterior median eyes, **SC1-3** soma cluster 1-3.

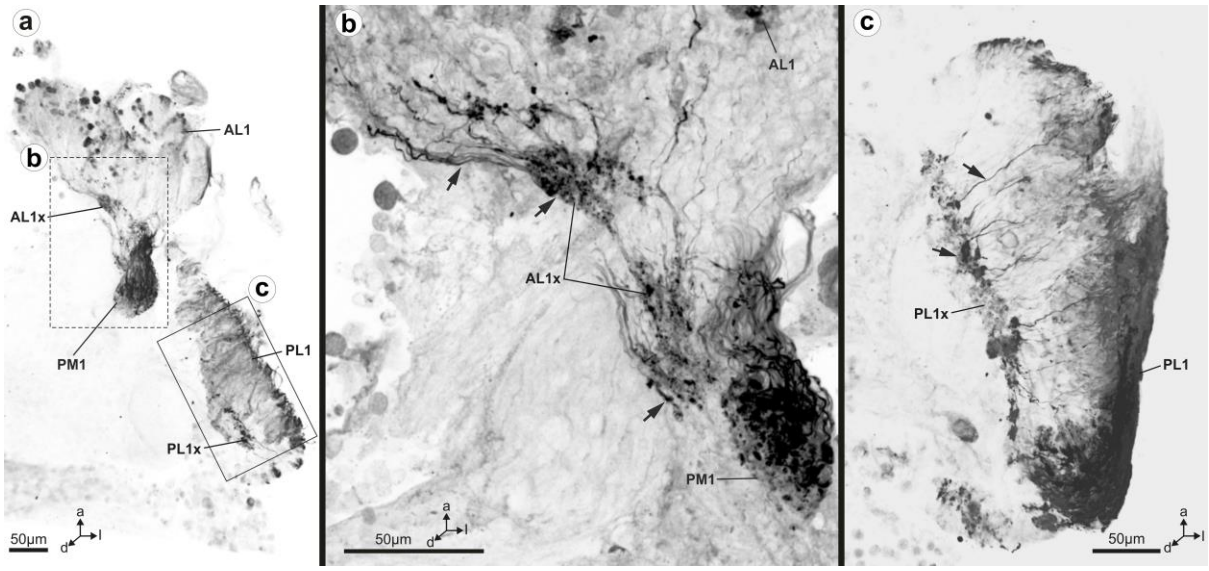

Figure 8. Maximum projections of image stacks (clsm), showing histamine-immunoreactivity in horizontal sections through the anteriormost protocerebrum of *Marpissa muscosa*. **a** Overview, shows strong histamine-immunoreactivity of retinula cell axon terminals in the AL1 and its substructure the AL1x, as well as in the PL1 and its substructure the PL1x. Retinula cell axons of the PME and their terminals in the PM1 exhibit strong histamine-immunoreactivity. **b** Magnification showing histamine-immunoreactive retinula cell axons and their terminals in the AL1x and PM1. Note the close spatial association of AL1x and PM1; AL1x is somewhat distorted due to sectioning. Arrows point to histamine-immunoreactive retinula cell axons and their terminals. **c** Magnification showing histamine-immunoreactive retinula cell axons and their terminals in the PL1 and PL1x. Arrows point to a retinula cell axon and a large terminal in the PL1x. **Abbreviations: a** anterior, **AL1** first order visual neuropil of the anterior lateral eyes, **AL1x** neuropilar subunit of the AL1, **d** dorsal, **l** lateral, **PL1** first order visual neuropil of the posterior lateral eyes, **PL1x** neuropilar subunit of the PL1, **PM1** first order visual neuropil of the posterior median eyes.

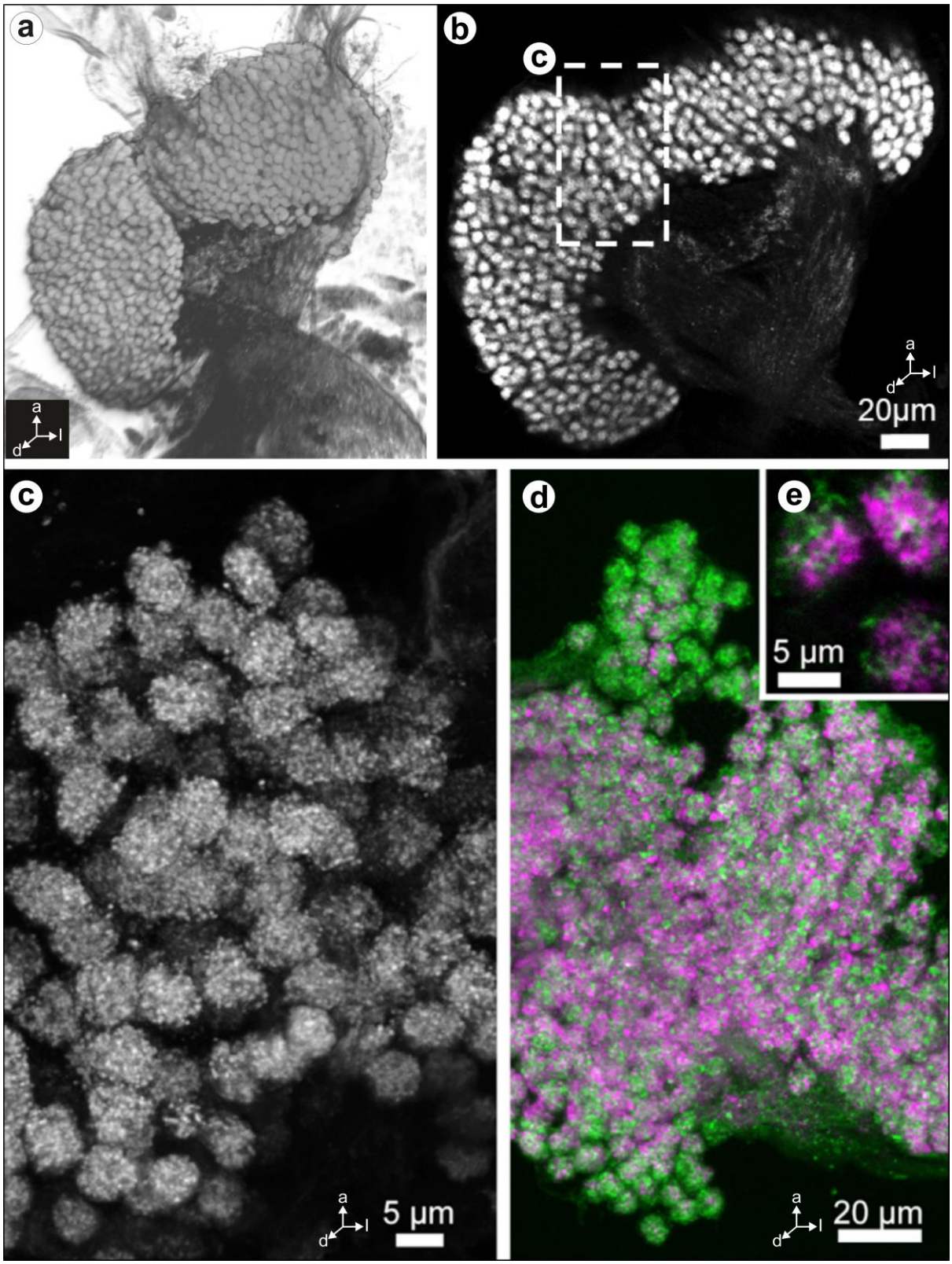

Figure 9. The second order visual neuropil of anterior lateral and posterior lateral eyes in the secondary eye visual pathway of *Marpissa muscosa.* **a** Three-dimensional volume rendering of an anti-synapsin labeled whole-mount, view from posterodorsal. Note the two distinct clusters of glomeruli that adjoin closely and coat the MBp anteriorly. **b** Single optical section of the AL2/PL2 within an anti-synapsin labeled whole-mount shows two distinct clusters of AL2/PL2 and a chiasm of neurites connecting them to the MBp. **c** Stack of optical sections

through the AL2/PL2 (maximum intensity projection), showing synapsin-immunoreactivity. The glomerular subunits within each individual AL2/PL2 may represent synaptic boutons. **d** Anti-synapsin (magenta) and phalloidin (green) double–labeling reveals glomerular substructures (boutons) of the AL2/PL2. **e** Three individual AL2/PL2 with glomerular substructures (boutons) labeled by anti-synapsin and phalloidin.

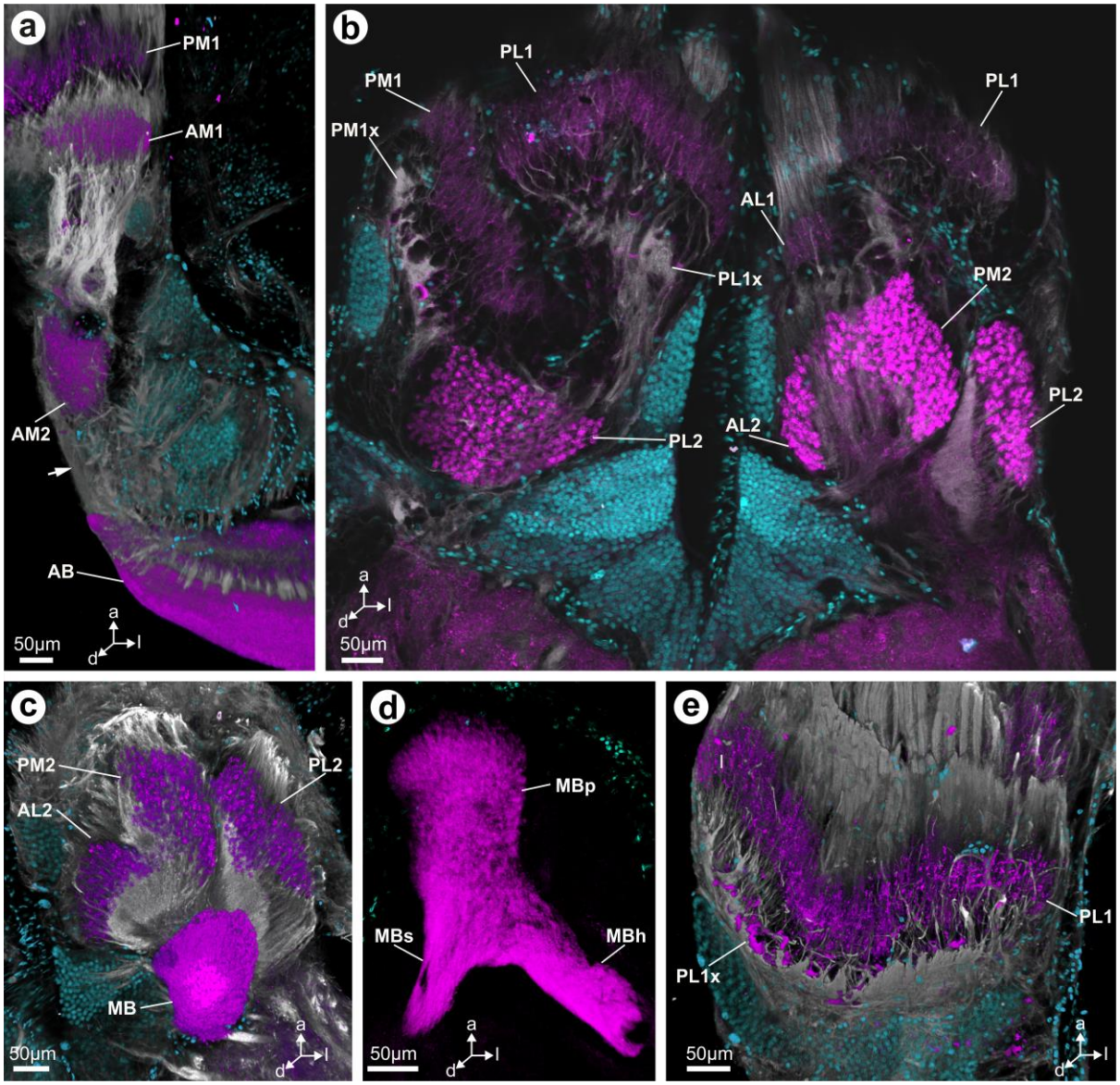

Figure 10. Maximum projections of image stacks (clsm; **a,c-e**) and single optical section (clsm) showing synapsin-immunoreactivity (magenta), tubulin-immunoreactivity (grey) and somata (cyan) in the secondary eye visual system of *Cupiennius salei*. **a** In the principal eye visual pathway, the AM1 is connected to the AM2 via a thick tract. Connecting neurites between AM2 and the AB are also visible (arrow). **b** Within the secondary eye visual pathways, every eye is associated with its own first order visual neuropil (AL1, PM1 and PL2); the PM1 and PL1 appear to have a substructure (PM1x and PL1x). All three second order visual neuropils are sub-structured into glomeruli. **c** The AL2, PM2 and PL2 are all connected to the MB. **d** The MB of *C. salei* consists of a MBp, MBh and MBs. All three substructures form a continuous synapsin-rich neuropil. **e** Horizontal section showing the PM1 and the PM1x. **Abbreviations: a** anterior, **AB** arcuate body, **AL1** first order visual neuropil of the anterior lateral eyes, **AL2** second order visual neuropil of the anterior lateral eyes, **AM1** first order visual neuropil of the anterior median eyes, **AM2** second order visual neuropil of the anterior median eyes, **d** dorsal,

l lateral, **MBh** mushroom body haft, **MBp** mushroom body pedunculus, **MBs** mushroom body shaft, **PL1** first order visual neuropil of the posterior lateral eyes, **PL1x** neuropilar subunit of the PL1, **PL2** second order visual neuropil of the posterior lateral eyes, **PM1** first order visual neuropil of the posterior median eyes, **PM1x** neuropilar subunit of the PM1, **PM2** second order visual neuropil of the posterior median eyes.

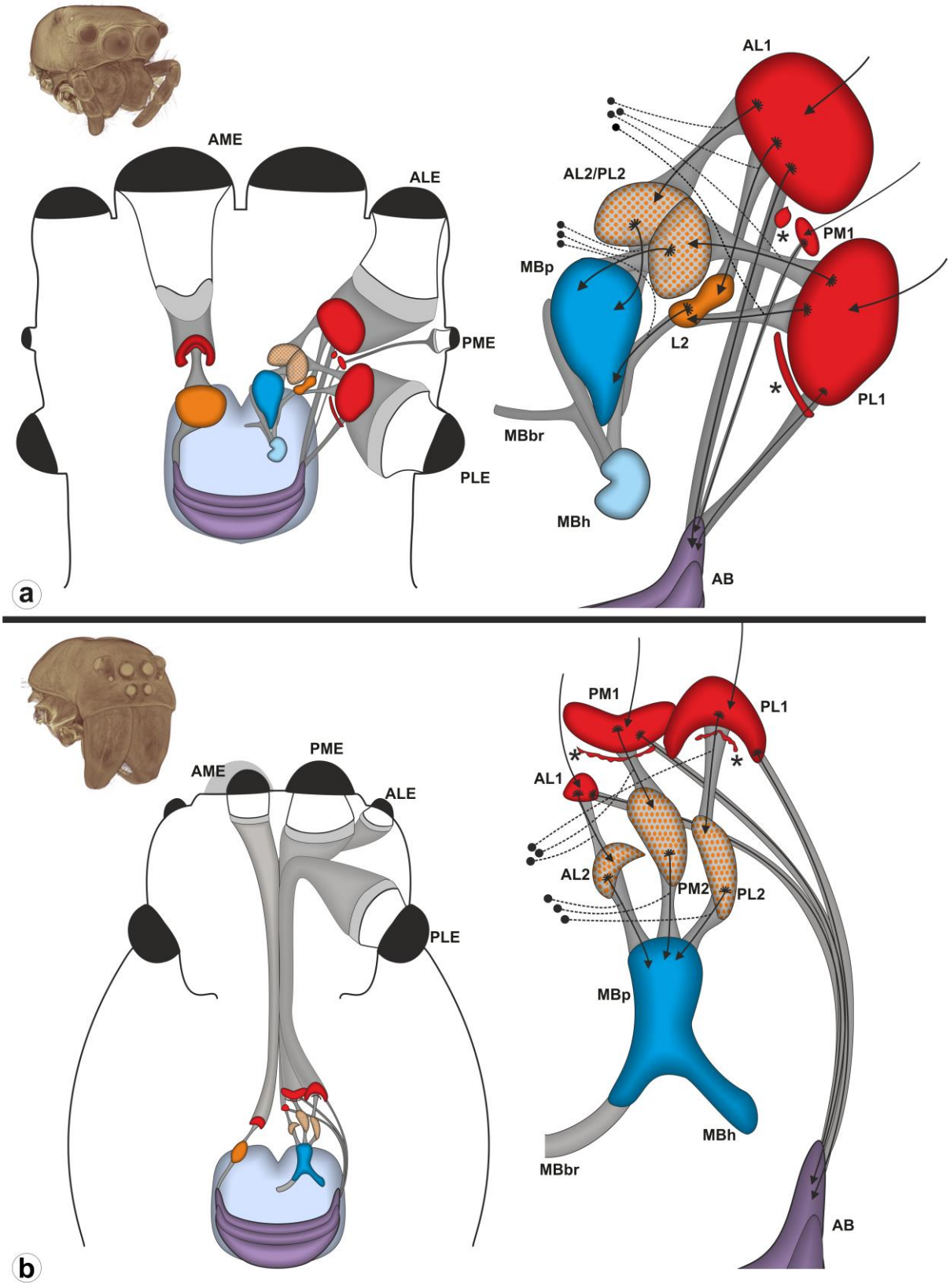

Figure 11. Schematic representations of the principal and secondary eye visual pathways in the brains of **a** *Marpissa muscosa* and **b** *Cupiennius salei.* Insets top left: 3D volume rendering of the prosomata of **a** *M. muscosa* and **b** *C. salei*, based on microCT analysis. **b** Left anterior median eye concealed by posterior median eye. **Abbreviations: AB** arcuate body, **AL1** first order visual neuropil of the anterior lateral eyes, **AL2** second order visual neuropil of the

anterior lateral eyes, **AL2/PL2** second order visual neuropil of anterior lateral and posterior lateral eyes, **ALE** anterior lateral eye, **AME** anterior median eye, **L2** shared second order visual neuropil of the anterior lateral and posterior lateral eyes, **MBbr** mushroom body bridge, **MBh** mushroom body haft, **MBp** mushroom body pedunculus, **PL1** first order visual neuropil of the posterior lateral eyes, **PL2** second order visual neuropil of the posterior lateral eyes, **PLE** posterior lateral eye, **PME** posterior median eye, **PM1** first order visual neuropil of the posterior median eyes, **PM2** second order visual neuropil of the posterior median eyes. **Filled black circles** indicate somata with known positions, **dotted lines** represent primary neurites and **arrows** indicate the assumed direction of information flow. **Asterisks** mark neuropilar subregions of first order neuropils (AL1x and PL1x in *M. muscosa*, PM1x and PL1x in *C. salei*).